معهد
الملك عبدالله
للبحوث والدراسات الاستشارية
KAI-RCS

www.kai.org.sa
e-mail:info@kai.org.sa

Final Report on

SEISMIC ACCELERATION CONTOUR MAPS (KSU)

[Contrat No. 6600011180]

By: King Abdullah Institute for
Research & Consulative Studies

July 2006

Final Report

On

SEISMIC ACCELERATION CONTOUR MAPS (KSU)

(Contract No. 6600011180)

Study Team:

1. **Dr. Mohamad S. Al-Haddad**
2. **Dr. Rajeh Al-Zaid**
3. **Dr. Abdulrahim Arafah**
4. **Dr. Abdullah Al-Amri**
5. **Dr. Tariq Al-Khalifa**

Senior Engineering Consultant:
Khaled M. Al-Sheref
Consulting Services Department
Saudi Aramco, Dhahran

July 2006

Table of Content

CHAPTER 1
INTRODUCTION

This Final Report on the Study "SEISMIC ACCELERATION CONTOUR MAPS (KSU)", (contract No. 51096/00) culminates the work reported in seven progress reports. The main objective of the study is to furnish the Saudi Building Code by mapped maximum considered earthquake spectral response accelerations at short period "S_s" & long period "S_1" for the Kingdom. Saudi Aramco specified the required works, in Section 3.2 of SCHEDULE B of the contract, as follows:

1- Reassessment of seismic hazard considering the most recent seismicity of the Kingdom of Saudi Arabia and neighbouring countries
2- Derivation of design ground motion parameters (maximum considered earthquake spectral response acceleration at short period "S_s" & long period "S_L" consistent with IBC-03 (NEHRP 2000).
3- Provision of two separate drafts 8.5" X11" colour figures in hard copy for mapping contours of the nodes values of S_s & S_L. superimposed on the Kingdom's geographic map.
4- Provision of values of accelerations S_s & S_L for each major city in Kingdom in table and electronic format.
5- Provision of final (checked) 8.5" X11" colour figures in hard copy and electronic format for mapping contours of the nodes values of S_s & S_L superimposed on the Kingdom's geographic map.
6- Provision of suggested modifications to pertinent IBC-03 sections based on this study.
7- Preparation of the scaled response spectra for producing design loads.
8- Provision of a draft of the Final Report.
9- Provision of Final Report in hard copy and electronic formats.

The efforts and the methodology that were undertaken to achieve the objectives of this study was initiated with interrelated multidisciplinary geological, seismological, and seismotectonic studies of seismic sources that may be of significant effects on evaluation of seismic hazard in the Kingdom. The main tectonic features and geologic structures of the Kingdom were analyzed

and characterized in term of their components of potential seismic faults and their effect on the seismic hazard. The efforts pertained to these study also involved compilation of up to date comprehensive earthquake catalog of the Kingdom and neighbouring countries. The earthquakes catalog was superimposed on the designated tectonic framework of a recent seismo-tectonic map of the Kingdom, which provides the basis of the probabilistic modeling for assessment of seismic hazard of the study. The seismo-tectonic map was analyzed and regionalized to 21 main zones (areas) that have relatively homogeneous seismotectonic characteristics. The map also shows the various potential seismic faults that were assigned to each designated zone. The geometry and style of main faulting system are tabulated. Independent earthquake database then was compiled for each designated seismic sources. The databases were subjected to treatment and seismological analysis for: identification and elimination of duplicated events and clusters, missing magnitude, completeness of the catalog. The earthquake recurrence analysis was then performed for each seismic source based on its respected final database.

Another of equal important step the study methodology pertained to selection of an appropriate ground motion Attenuation Relationship (AR) for use of the probabilistic seismic hazard assessment. Several AR,s have been examined and compared with ground motion acceleration data recorded during 1995 Gulf of Aqaba Earthquake. The most relevant AR was found to be the refined version of the relationships of Sadigh et al (1989) and Sadigh and Chang (1990).

To this end, all input parameters for earthquake hazard analysis at all study sites were been furnished. The AR table along with the geometry and seismic characteristics of the designated seismic courses were incorporated in computer modeling for probabilistic seismic hazards analysis. The earthquake recurrence parameters of the respected sources were assigned for the different sources based on an inherent uncertainties logic tree distribution. As per the recommendations of section 4.1.3 of NEHRP (2000), the spectral response of ground motion accelerations with 2% probability of being exceeded in 50 years were calculated for two levels of longitude-latitude grids. The first grid model is referred to thereafter as (Country Model) and the second model is referred to thereafter as (Regional Model). The results of the Country Model were used for contouring the response spectral accelerations at short period (0.2 second) (S_S), and at 1-second on the whole geographical map of the Kingdom. The Regional Model results were used to produce maps of (S_S) and (S_1) with lower contouring levels for 7 separate parts of the Kingdom map. All maps are given in Chapter 4.

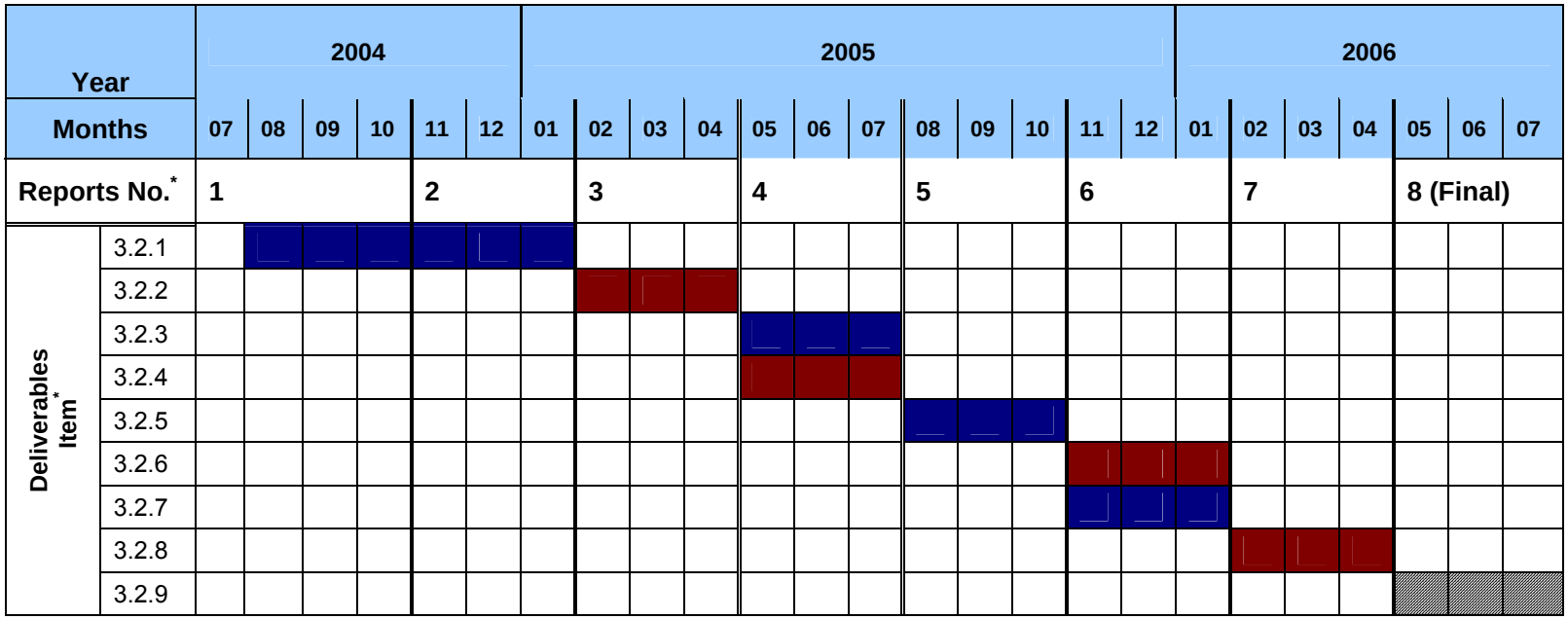

* See Table 1.2

** See Table 1.3

Table 1.3 Deliverables as Prescribed in 3.2 of SCHEDULE "B".

Deliverable	Description
3.2.1	Reassessment of seismic hazard considering the most recent seismicity of the Kingdom of Saudi Arabia and neighboring countries.
3.2.2	Derivation of design ground motion parameters (maximum considered earthquake spectral response acceleration at short period "S_s" & long period "S_L" consistent with IBC 2003 (NEHRP 2000).
2.2.3	Provision of two separate drafts 8.5" X11" colored figures in hard copy for mapping contours of the nodes values of S_s & S_L. superimposed on the Kingdom's geographic map.
3.2.4	Provision of values of accelerations S_s & S_L for each major city in Kingdom in table and electronic format.
3.2.5	Provision of final (checked) 8.5" X11" colored figures in hard copy and electronic format for mapping contours of the nodes values of S_s & S_L superimposed on the Kingdom's geographic map.
3.2.6	Provision of suggested modifications to pertinent IBC-2003 sections based on this study.
3.2.7	Preparation of the scaled response spectra for producing design loads.
3.2.8	Provision of a draft of the Final Report.
3.2.9	Provision of Final Report in hard copy and electronic formats.

CAHPTER 2

SEISMOTECTONIC SETTING AND REGIONAL SEISMICITY

2.1 General

In the statistical characterization scheme for the seismogenic source zones of the eastern Arabian Peninsula, different set of seismic data corresponding to two period of observation were utilized. The set of observation period were: 112 – 1964 AD and 1965-2003. The first set is labeled as historical data while the second set is instrumental data for purposes of discussion. The source catalogues from which the utilized seismic data are taken were the United States Geological Survey (USGS) PDE/EDR: 1963-2003; the International Seismological Center (ISC): 1963-2003: Ambraseys (1988) from 112-1963 AD; the European Mediterranean Seismological Center (EMSC): 1990-2003; the Seismic Studies Center (SSC) of King Saud University from 1986-2002, and the Kuwait National Seismological Network (KNSN) from 1997-2003. The seismic data obtained from these different seismic bulletins were merged and compiled to provide the main database for delineation and identification of the different seismogenic source zones in eastern Arabian Peninsula and for statistical analysis. The compiled seismic data were likewise utilized in the seismotectonic correlation of the activity in each source area. Different types of magnitude such as surface-wave (Ms), body-wave (Mb), local (Ml), duration (Md), macro (Io), and others were converted to two types which are the surface-wave and body-wave to homogenize the main database. The purpose of homogenizing the database is due to the appropriateness of using the Ms in the concept of seismic moment, while the Mb for the seismicity parameters.

In the delineation and identification of the seismogenic source zones in eastern Arabian Peninsula, some criteria were followed and utilized as guidelines. These are:

- Seismological parameter – map of the space-time distribution of seismic events that could indicates the seismogenic provinces and seismoactive faults, and occurrence of large earthquakes, the level of which depends upon the seismic activity in the region.
- Geological parameter – map of regional tectonics in the area which indicates the location of joints, faults, lineaments, and rift systems that are associated with seismic activities.

The boundaries of the seismogenic source zones are the results in the inter-agreement of these two criteria with the higher priority given to the spatial distribution of epicenters due to statistical needs in statistical analysis. The seismogenic source zones are selected that are composed of systems of faults or lineaments or rift systems whose boundaries do not traverse generally other tectonic units. Some of the seismogenic source zones are relatively large due to scarcity of earthquakes in this part of the eastern Arabian Peninsula. From these considerations, there are twelve (12) seismogenic source zones that were identified and delineated. These are:

Seismic Source Zone Number	**Name of Source Zone**
14	Sirhan-Turayf-Widyan Basins
15	Najd Fault Zone
16	Central Arabian Graben Zone
17	Arabian Gulf
18	Zagros Fold Zone
19	Sanadaj-Sirjan Ranges
20	Eastern Yemen
21	Rub Al Khali-Ghudun Basins
22	Dibba-Bandar Abas Region
23	Hawasina-Makran Thrust Region
24	East Sheba Ridge
25	Masirah Fault System

The characterization of the seismogenic source zones of eastern Saudi Arabia is composed of two parts that are similar to the scheme of composition of the western section. These are the brief discussions covering the possible association of each source zone to the tectonic and seismicity in each source area. There are two tectonic sources assumed in each source zone. These are the fault and area sources whose seismic activities are combined to determine the seismicity level using the frequency-magnitude relation. Under the fault source, all types of faults whenever possible are included. Area source is defined to be dislocations found to be off the fault source. The other part is a logic tree diagram for graphical description of the physical and seismicity parameters involved in seismotectonic correlation.

2.2 Regional Tectonics

The accretionary evolution of the Arabian plate is thought to have originated and formed by amalgation of five Precambrian terranes. These are the Asir; Hijaz, and Midyan terranes from the western part of the Arabian shield, and from the eastern side of the shield are the Afif terrane and the Amar arc of the Ar Rayn micro-plate. The western fusion is along the Bir Umq and Yanbu sutures (Loosveld et al 1996). The eastern accretion may have started by about 680-640 million years ago (Ma) when the Afif terrane collided with the western shield along the Nabitah suture. At about 670 Ma, a subduction complex formed west of Amar arc. Along this subduction zone, the Afif terrane and Ar Rayn microplate collided that lasted from about 640-620 Ma. The north trending Rayn anticlines and conjugate northwest and northeast fractures and faults may have formed at this time (Husseini 2000) (Fig.2.1).

The regularly spaced north trending Summan platform, Khurais-Burgan and En Nala-Ghawar anticlines, and Qatar arch in the eastern part of the Arabian plate appear to have formed during the Precambrian Amar Collision about 640-620 million years ago (Ma). This collision occurred along the north trending Amar suture that bisects the Arabian peninsula at about 45 degrees east longitude when the Rayn microplate in the east was fused to the western part of the Arabian craton (Husseini 2000, Looseveld et al 1996, Ziegler 2001). The great anticlines are bounded by the northeast trending Wadi Batin fault and northwest trending Abu Jifan fault that converge on the Amar suture. The anticlines intersected deformed metasediments that are dated as syn-collisional. The Amar collision was followed by a widespread extensional collapse of the Arabian-Nubian shield between about 620-530 Ma. The extensional collapse culminated in the regional development of the extensive Najd fault and its complimentary rift basins, Zagros suture, the northeast trending Oman salt basins, Dibba fault, and the Sinai triple junction. The Sinai triple junction is composed of the Najd fault system, the Egypt rift, the Jordan valley, and Derik rift (Stern & Hedge 1985, Bender 1982, Andrews 1991). During the final extensional stage about 530-570 Ma, the northwest trending Najd fault system dislocated the Arabian shield left-laterally by about 250-300 kilometers. This dislocation appears to compliment the northeast oriented intra-continental rifts in Oman, Zagros mountain, and the Arabian gulf. These rift basins

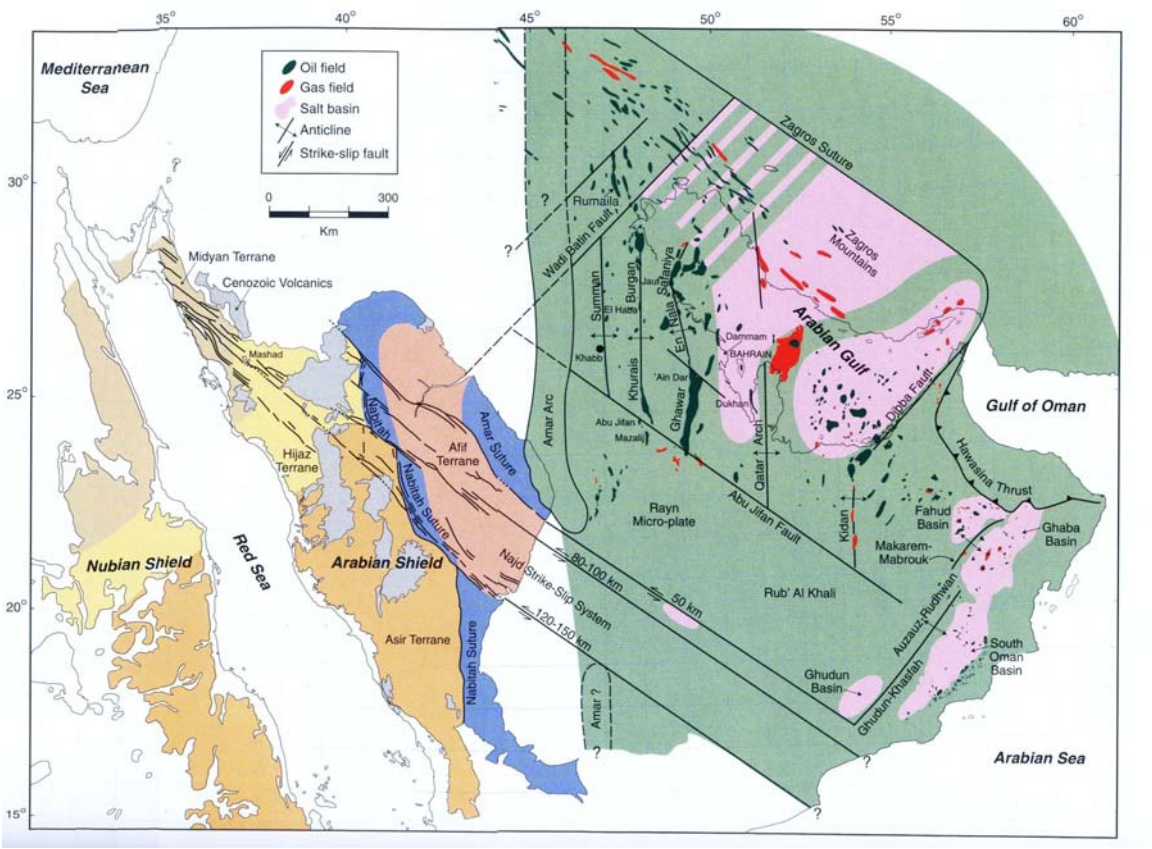

Fig. 2.1 : The terranes, and Amar Arc of the Rayn micro-plate. The Rayn micro-plate (Green) forms the eastern part of the Arabian Plate (Husseini, 2000).

accumulated thick sequences of clastic and carbonate rocks and salt such as the Ara group in Oman, Hormuz series in the Arabian gulf and Zagros mountain (Ziegler 2001). During the extensional collapse, the north trending anticlines probably remained elevated as elongated horst bounded by normal faults. The intervening subsiding grabens accumulated syn-rift sediments including the Hormuz salt, and form an inter-fingering pattern between the great north trending anti-clines

(Fig.2.2).

The striking geometric pattern appears to have formed in two tectonic stages. The Precambrian Amar collision between about 640 and 620 Ma followed by the development of the Najd rift system between about 570-530 Ma.

In Oman, during the intra-extensional tectonics (rift cycle 1), a series of north-south to northeast –southwest trending basement highs may have developed from north to south. These are the Ghudun-Khasfah high, the Anzaus-Rudhwan Ridge and the Makarem-Mabrouk high, separating different basin segments. The event is also associated with igneous activity which is the

formation of the Oman Mountains and is followed by a thermal subsidence phase. During this cycle, there may have been widespread rifting of the Abu Mahara group (During the Cambrian to mid-Carboniferous (Rift Cycle 2), the Abu Mahara rift configuration was reactivated. The re-activated eastern angle low-angle bounding fault of the Ghudun-Khasfah high becomes the western margin of the asymmetrical South Oman basin. In the north, the Ghaba salt basin develops as a narrower, deeper and asymmetrical feature with some asymmetry reversals. The South Oman and Ghaba salt basins are related to the Najd event of rifting and wrenching dated at between 600-540 Ma (Looseveld et al 1996). Around 110 Ma, the Atlantic ocean started to open, leading to the closure of the Neo-Tethys between the Afro-Arabian and Eurasian plates. A northeasterly dipping intra-oceanic subduction zone developed, accompanied by back-arc spreading. At approximately 93 Ma, this subduction complex collided with the continental crust of Oman. Uplift and partial erosion of the Natih formation and the development of a major hardground signaled the onset of this event. The initial onset has been described as a mobile or stationary (Robertson 1987, Nolan et al 1990) fore-bulge that preceded down-warping of the foreland ahead of the advancing thrust front. During this phase, the Hawasina and Samail Nappes are emplaced, the region south of the nappes are down warped with local footwall uplift, the Aruma foredeep develops, a dextral transtension along the Fahud fault zone, and a sinistral transtension along the Maradi fault zone occur. In the Eocene-Pliocene second Alpine phase,

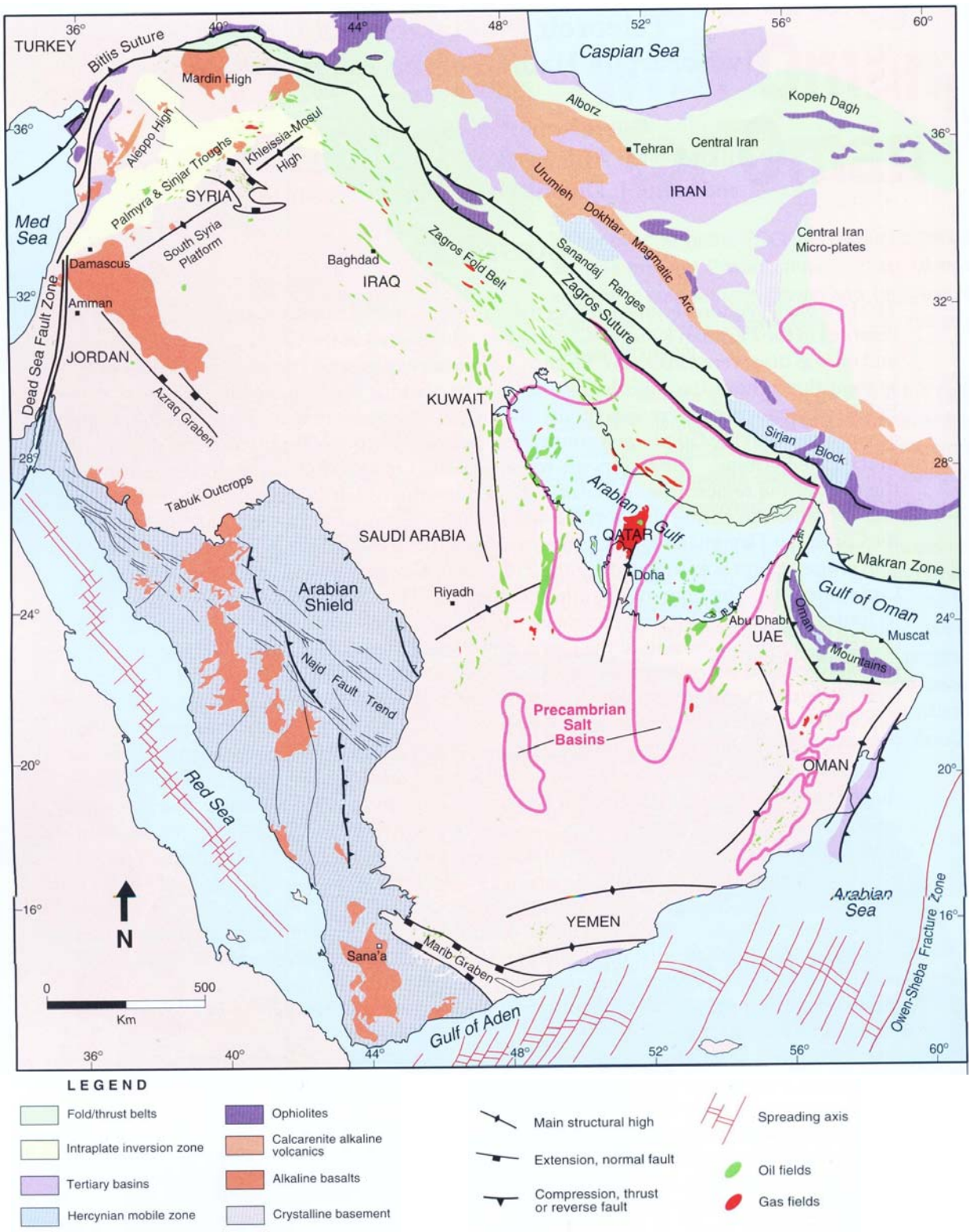

Fig. 2.2: Location and major tectonic elements of the Arabian plate and Iran. The Makran and Zagros separate the Arabian plate from the microplates of interior Iran.

folding commences in the Oman mountains and shortening overprints extension in the area around Natih, Fahud, and the northern Maradi fault zone (Noweir & Asharhan 2000). The Salakh arch develops, reverse faulting occur in foredeep, the northern portion of the Maradi fault zone is inverted in dextral transpression, and the Fahud main fault is re-activated with a small sinistral component.

At the Cretaceous-Tertiary boundary, intra-oceanic north-over-south thrusting between the lower and upper nappies of Masirah island occurred, immediately followed in the Paleocene by the oblique obduction of the Masirah complex onto the Arabian continent. Along the east coast of Oman, largely offshore under Masirah bay and Sawqrah bay, a narrow, gently folded foreland basin, the Masirah trough, developed. The western margin is bounded by normal faults reactivating Mesozoic rift related faults. On its eastern margin, a wedge of ophiolitic and probably continental slope sediments is largely under thrust below the eastern and uplifted part of this fore deep basin.

2.3 Regional Seismicity

The seismicity map of eastern Saudi Arabia involving both historical and instrumental earthquake data from magnitude 4.5 and above as shown in fig. 3.3 indicates a sparse distribution of seismic events in the Arabian Platform and western portion of the Arabian Craton. In the northwestern part, two seismic events are located at Harrat al Harrah, one at Umm Wuai graben and two at the Widyan basin. At the central portion of the Arabian shelf, three earthquake events are shown to be positioned among the great anticlines (Summan platform, Khurais-Burgan and Ghawar-En Nala anticlines, Qatar arch) that are bounded by the Wadi Batin and Abu Jifan faults. In the Arabian gulf from the Hormuz salt basin up to the Mesopotamian foredeep of southern Iraq shows also sparse distribution of epicenters, Southeastward of the Arabian shield and south of the central part of the Arabian shelf, three seismic event have epicenters in the Rub Al-Khali basin and two more in the Hadramaut arches in eastern Yemen. In Oman, two seismic events are located in the Hawasina thrust sheet, while the others are along the Dibba fault and the Makran-Zagros subduction zone. This subduction zone is the only region where an oceanic lithosphere is being subducted, where apparently the oceanic crust in the gulf of Oman is being consumed beneath southern Iran. To the southeast of Oman, along the Masirah trough zone gives one earthquake event. Down south, a spatial concentration of seismic events can be seen. This distribution is in the East Sheba ridge which is between the Alulak-Fartak trench in eastern Yemen to the west and the Owen fracture zone to the east. The ridge is also between the Socotra Island in the south and the Masirah trough in the north. The ridge is part of

a line of epicenters that connects the gulf of Aden to the west and the Carlsberge ridge to the south.

However, there is an increasing concentration of earthquake epicenters going toward the northeast directions of the Arabian platform and the zone of convergence below the southwestern direction of Lut block in Iran and parallel to the Oman line. One of the concentrated spatial distributions of seismic events is shown to occur in the Zagros Mountains folded belt that extends for a distance of about 1500 km in a northwest-southeast direction. The simple folded belt is an area of about 250 km in width. The earthquakes in the Zagros folded belt define a zone of about 200 km wide that runs parallel to the fold belt. The majority of earthquakes occur in the crustal part of the Arabian plate that is subducted along the folded belt. Magnitude 5 earthquakes are frequent and magnitude 6 may occur sometimes yearly. This tendency of increasing seismicity thins out in the Main Zagros Thrust (MZT) and the Sanandaj-Sirjan ranges in Iran.

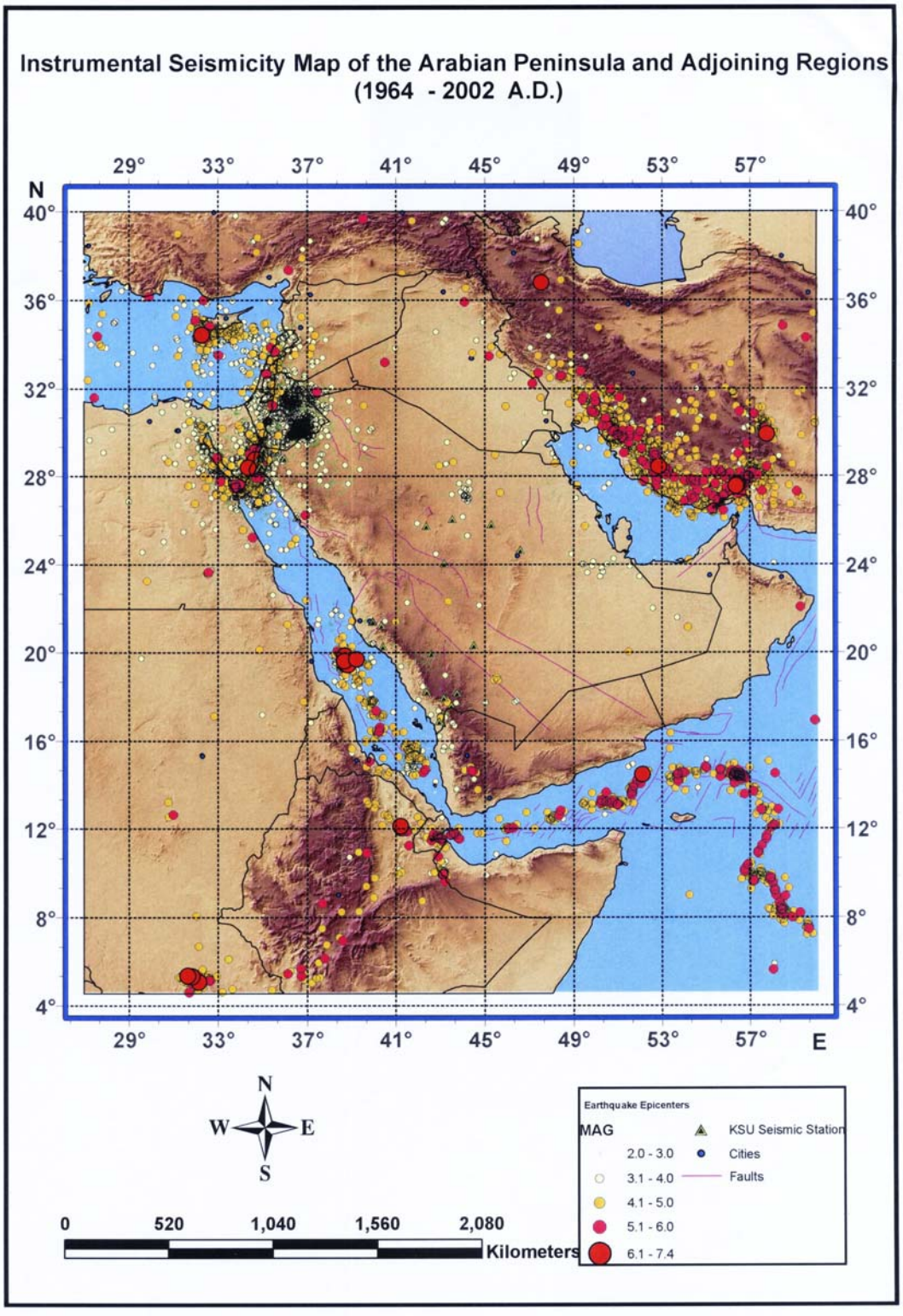

Fig. 2.3 Regional Seismisty of the Study Area

CHAPTER 3
SEISMOGENIC SOURCE ZONES

3.1 Regionalization of Seismic Zoning

The characterization of the seismogenic source zones is composed of two parts. These are the brief discussions covering the possible association of each source zone to the tectonic and seismicity model of the areas contained in each source zone. The other part is a logic tree diagram for graphical description of the physical and seismicity parameters involved in seismotectonic correlation.

Two methods of approach were employed in the study. These are seismicity and fractures. Under the seismicity approach, the set of seismic data in each source zone was utilized to plot the magnitude-frequency relation, and for the estimation of the linear seismic slip and seismic moment release rates. From the frequency graphs, the respective seismicity parameters were determined for correlation to tectonic structures and probable earthquake source mechanisms. Under the second approach, the tectonic structures contained in each source zones were examined based on existing geological/tectonic maps for identification and association to the types of earthquake source mechanisms, and to the seismicity of the source area. Combination of the two approaches leads to the preliminary framework of a seismotectonic model for each seismogenic source zone.

From the findings, there were at most two types of sources for the tectonic model. These are the fault and area source. Under the fault source are the transcurrent and normal faults and their respective variations. Under the area source are the seismic events not directly associated to known presence of fractures or are off located, and or the sudden or randomly distributed dislocations of the ground within the source zones. Presumably, the causes of these seismic events under the area source are due to lateral and vertical structural discontinuities, or connected to some anomalous behavior of geophysical phenomena, and or undetected fractures.

For earthquake source mechanisms, there are also at most two types. These are the extrusion and transcursion mechanisms. The zones of extrusion are the seats of volcanic activity and high heat flow. Seismological and other geophysical data suggest that ridges and their continental extension are characterized by rifting, spreading, and other aspects of extensional tectonics. Other earthquakes observed in eastern Saudi Arabia are those that probably belong to the intraplate population. Intra-plate faults have slow slip-rate, shorter in fault length and more discontinuous, and have long recurrence time intervals. These characteristics of intra-plate faults in relation to seismicity are mostly observed among seismic events that have occurred in some

parts of the shield areas.

Generally, in the delineation and identification of the seismogenic source zones in eastern Arabian Peninsula, some criteria were followed and utilized as guidelines. These are:

1. Seismological parameter – map of the space-time distribution of seismic events that could indicates the seismogenic provinces and seismoactive faults, and occurrence of large earthquakes, the level of which depends upon the seismic activity in the region.
2. Geological parameter – map of regional tectonics in the area which indicates the location of joints, faults, lineaments, and rift systems that are associated with seismic activities.

The boundaries of the seismogenic source zones are the results in the inter-agreement of these two criteria with the higher priority given to the spatial distribution of epicenters due to statistical needs in statistical analysis. The seismogenic source zones are selected that are composed of systems of faults or lineaments or rift systems whose boundaries do not traverse generally other tectonic units. Some of the seismogenic source zones are relatively large due to scarcity of earthquakes in this part of the eastern Arabian Peninsula. From these considerations, there are twelve (12) seismogenic source zones (Fig. 3.1) that were identified and delineated. These are:

Table 3.1 Seismogenic Source Zones of Central & Eastern Arabian Peninsula

Zone No.	Name	Cooridinates		Area (KM^2)
		Lat. N	Long. E	
14	Sirhan-Turayf-Widyan Basins	32.28	36.48	343516
		32.01	47.13	
		26.46	41.72	
		28.29	39.75	
15	Najd Fault Zone	28.29	39.5.75	379730
		20.62	48.36	
		17.32	45.27	
		20.2	43.1	
		23.33	41.75	
16	Central Arabian Graben Zone	26.46	41.72	533174
		30.86	46.02	
		23.52	51.46	
		20..62	48.36	
17	Arabian Gulf	30.86	46.02	257798
		32.01	47.13	
		25.96	54.17	
		23.52	51.46	
18	Zagros Fold Belt	32.01	47.13	160644
		32.01	50.11	
		27.31	55.6	
		25.96	54.17	
19	Sanandaj-Sirjan Ranges	32.01	50.11	148636
		32.0	53.84	
		28.8	57.3	
		27.31	55.6	
20	Southern Yemen	17.32	45.27	408636
		20.62	48.36	
		16.12	54.0	
		13.66	46.18	
21	Rub Al Khali-Ghudun Basins	20.62	48.36	403580
		24.16	52.22	

Zone No.	Name	Cooridinates		Area (KM^2)
		Lat. N	Long. E	
		19.69	57.32	
		16.12	54.0	
		18.02	55.62	
22	Bandar Abbas-Dibba Region	24.16	52.22	140096
		28.8	57.3	
		27.5	58.48	
23	Makran-Hawasina Thrust Zone	22.85 22.85	53.76 53.76	324060
		27.5	58.48	
		24.88	61.68	
		19.69	57.32	
24	East Sheba Ridge	16.12	54.0	209585
		18.02	55.62	
		14.09	59.46	
		11.99	57.44	
		14.05	54.61	
25	Masirah Fault Zone	18.02	55.62	238136
		24.88	61.68	
		14.09	59.46	
		19.69	57.34	

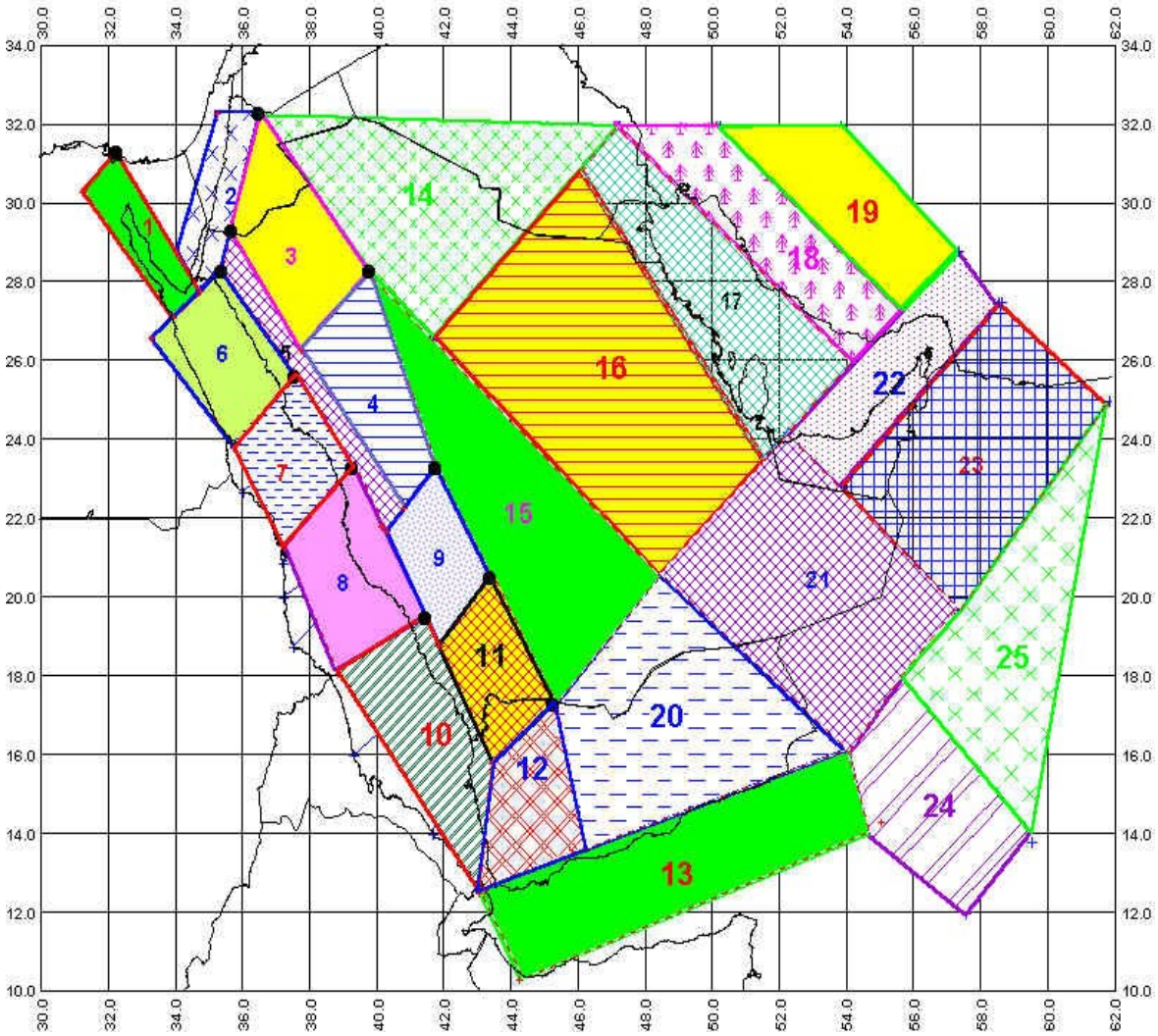

Fig. 3.1 Seismic Source Zones Regionalization
of the Arabian Peninsula and Adjoining Regions

Generally, the characterization of the seismogenic source zones of eastern Saudi Arabia is also composed of two parts that are similar to the scheme of composition of the western section. These are the brief discussions covering the possible association of each source zone to the tectonic and seismicity in each source area. There are two tectonic sources assumed in each source zone. These are the fault and area sources whose seismic activities are combined to determine the seismicity level using the frequency-magnitude relation. Under the fault source, all types of faults whenever possible are included. Area source is defined to be dislocations found to be off the fault source. The other part is a logic tree diagram for graphical description of the physical and seismicity parameters involved in seismotectonic correlation. Symbolism is used in each logic tree diagram. These are as follow:

Mmax( ) – expected maximum magnitude. Letter inside parenthesis means the source from which Mmax is taken. Letter S is for seismicity, O from observation, L from fault length, and A for assigned.

a and **b** – seismicity parameters as obtained from cumulative frequency-magnitude relation and or (Utsu 1965 and Aki 1965) maximum likelihood estimate method.

ASSR – average seismic slip rate in mm/yr

ASMoR – average seismic moment release rate in dyne-cm/yr

P – relative frequency or assigned probability due to distribution or location of seismic events in each source zones. Number inside parenthesis indicates assigned value.

TrDmax – approximate recurrence time in years of the maximum dislocation corresponding to Mmax.

TrMo(max) – approximate repeat time in years of an earthquake population with a Mmax.

Hmax – crustal depth of structures corresponding to Mmax.

Pr – estimated probability of occurrence in 100 years of Mmax.

3.2 Seismic Sources Modeling

The empirical and theoretical correlation methods and distribution function that were applied in the western part of Saudi Arabia seismogenic source zones are similarly utilized for the eastern section. This approach is conducted to maintain uniformity and homogeneity of results.

The seismotectonic modeling of the seismogenic source zones of eastern Arabian Peninsula were based on the following empirical and theoretical correlations. The empirical correlation was taken from observation of earthquakes occurring in tectonic structures (Gubin 1967; Allen 1975). These are as follows:

3.2.1 Correlation between seismic and tectonic data

(a) Earthquakes do not occur everywhere, but only in definite tectonically active areas and in strong accordance with movement and deformation of geological structures. Globally, there were close relation between active faults and strong earthquakes, but the relations are not so strong in other areas characterized by less long term seismicity. The Earth is partitioned among large seismogenic and aseismogenic belts, which are apportioned further into smaller source zones. The seismogenic source zones have active faults at different depths, concealed in the depth or exposed on the surface. A seismogenic zone is therefore a main unit that determines the seismic conditions of a territory. The source zones are of different size and kind. In every zone occur earthquakes up to a definite value of the seismic parameters. These are due to varying size, degree of competency, and rate of movement, so that earthquakes correspondingly vary with the parameters.

(b) Major earthquakes occur along tectonically active source zones having large faults. The zones which divide geological units having different history of development and large difference in rates of movement are the most seismically active. The larger is the disturbed structure and the greater is its competency, the larger is the fault plane affected by the abrupt movements and the sronger will be the earthquake. Correspondingly, every group of homogeneously disturbed structure with definite competency and size has a definite ceiling of magnitude value. The more is the rate of structure movements along a fault and the less is the competency of these structures, the more rapidly the stress needed for an abrupt displacement of a structure along a fault is accumulated and the more often arise earthquakes of the maximum magnitude value for this structure. Every tectonically active source zone has its own rate of movement along it and corresponding frequency of earthquake occurrences.

(c) Geological structures move abruptly on faults along tectonically homogeneous active zone not simultaneously but alternatively in different places of the zones. Alternatively, in different places in this zone arise earthquake of maximum magnitude for this zone. When a source of an earthquake of certain maximum strength was recorded in this homogeneous active zone, then earthquake of the same strength can occur anywhere along this zone. In other word, the probability of such an earthquake can be extrapolated and interpolated along homogeneous tectonically active zones.

3.2.2 Correlation between Earthquake Frequency and Mechanics of Faulting

The geological interpretation of the mechanism of an earthquake could possibly was applied quantitatively by Reid in 1910 (Lomnitz 1987). The concept was extended by others (Haskell 1964; Burridge & Knopoff 1964; Keilis-Borok 1959) to establish the theoretical and physical correlation between occurrence of earthquakes and deformation of tectonic structures. The most important parameter in mechanics of faulting as related to occurrence of a seismic event is the seismic moment Mo (Aki & Richards 1980; Burridge & Knopoff 1964; Keilis Borok 1959)

Mo = uAD = uLWD (1)

where u is the rigidity, A is the fault plane area, L and W are the length and width of the fault respectively, and D is the displacement. The amplitude of the long period waves is proportional to the seismic moment. Since the surface magnitude (Ms) is calculated by measuring the amplitude of the long period wave, there exist a close relationship between Mo and Ms, and so with Mo, length and displacement arising from static similarity. For this study, the relationships are obtained empirically, which is a world-wide data collection of corresponding magnitude, moment, length, width and displacement. The empirical relationships that were obtained are as follows:

Log Mo = [(1.62+-0.112)Ms + 15.1] +-0.3 (2)

Log Mo = [(2.54+-0.087)Log L + 22.56] +-0.31 (3)

Log Mo = [(2.61+-0.28)Log D +26.32] +-0.44 (4)

From (2-4), the following equations can be obtained when the standard deviation and standard error of estimate are not incorporated

Log L = 0.64Ms – 2.94 (5)

Log D = 0.62Ms – 4.3 (6)

Equation (2) is within the range of values (1.5-1.7) as obtained by Kanamori (1977), Hanks & Kanamori 1979; Brune 1969; Scholz 1982; and Wyss (1973). Equations (5) and (6) are close to Matsuda (1975) results which are 0.6, 2.9: and 0.6, 4 for the coefficients and constants respectively. The rupture is assumed to take place in the entire length of the homogeneous part of the fault or portion for segmented fault. The constraining equations for the fault length, dislocation, and magnitude are from (2-4)

1.52LogD + 7.25 < Ms < 1.69LogD + 6.65 (7)

1.55LogL + 4.36 < Ms < 1.6LogL + 4.94 (8)

The magnitude frequency relation of earthquakes satisfies the empirical relation (Gutenberg & Richter 1954)

Log N = a – bMs (9)

where N is the number of magnitude Ms or greater, a and b the seismicity parameters. Equation

(9) holds down to the level of micro-events (Mogi 1962; Scholz 1968) which indicates a fundamental physical understanding of the fracture process can be known if the relation can be explained completely. The Mo and Ms are both measures of the strength of an earthquake, so that (9) can be expressed in terms of Mo by means of (2). The theoretical consideration that the magnitude scale saturates at higher values of magnitude, but not with Mo is appropriate to substitute the seismic moment frequency relation for characterizing earthquake occurrences. From (2) and (9), a power law size distribution of earthquakes can be obtained (Wyss 1973)

$$\mathbf{N(Mo) = Amo^{(-B)}} \qquad \mathbf{(10)}$$

$$A = \exp[(a + bc/d)\ln 10]$$

$$\mathbf{B = b/d}$$

where a and b, c and d are the constant and coefficient in (9) and (2) respectively. From Wyss (1973), the total moment of a given earthquake population is the integral

$$\mathbf{Mo(tot) = (AB/(1-B)[Mo^{(1-B)}]} \qquad \mathbf{(11)}$$

where the upper and lower limits of integration are Mo(max) and Mo(min) as the maximum and minimum seismic moment in a given earthquake population respectively. In (10) it is assumed that the Mo(max) is attained when N(Mo)=1, so that $A=Mo^B$. Likewise, in (9) the Mmax is also attained when N(M) =1. If Mo(min) is insignificant compared to Mo(max), (11) becomes approximately equal to

$$\mathbf{Mo(tot)= B/(1-B)Mo(max)} \qquad \mathbf{(12)}$$

From Wesnousky and Scholz (1983), the repeat time (Tmax) of (11) is

$$\mathbf{T(max) = Mo(tot)/Mo(g)} \qquad \mathbf{(13)}$$

where Mo(g) is the geologically assessed rate of moment release on a fault.

In (6), the recurrence time (Tmax) of an event with dislocation D is

$$\mathbf{T(max) = D/S} \qquad \mathbf{(14)}$$

where S is the linear average seismic slip rate.

The geologically assessed rate of moment release is not available in eastern Saudi Arabia. To be able to utilize the concepts enunciated in (9-14) for the correlation of regional seismicity to tectonics, there was a need to treat the 3 set of seismic data (historical, instrumental, recent) into one group in each seismogenic source zone in terms of Ms, to obtain the required parameters. The conversion equation was (Al-Amri et al 1998; Al-Amri 1994)

$$\mathbf{Ms = 1.14\ Mb\ -0.9} \qquad \mathbf{(15)}$$

where Mb is the body-wave magnitude.

Wesnousky and Scholz (1983) had indicated that the average geological moment release rate is almost the same as the average seismic moment release rate in 200-300 year of seismic data, and similar to the geological rate for 400 year of data. It is assumed then that the findings for seismic moment release rate have also the same similarities to the linear average seismic slip and or

spreading rate. The period of observation in each source zone is counted from the earliest recorded year of the data up to 2003.

The geologically assessed rate of moment release is assumed to be equal to the ratio of the cumulative seismic moment release and period of observation. This assumption was also applied to obtain the linear average seismic slip or spreading rate. The average slip rate in each zone with sufficient seismic data could be compared to other findings obtained from different sources for validation. If the seismic slip rates are compatible to other results, presumably the seismic moment release rates would also qualify. When sufficient data are not available, the other alternatives could be to assume the applicability of the other parameters obtained in neighboring seismic source zones and or using (12).

The expected maximum magnitude in each seismogenic source zone is either taken from (9) [Mmax(S)], or the observed maximum magnitude Mmax(O) from the set of seismic data in each source zone, and or the estimated magnitude [Mmax(L)] from fault length of the existing fractures in each respective seismogenic source zone. The expected Mmax(S) and or Mmax(O) are then correlated to fault length in (5) or dislocation in (6), and the magnitude from crustal depth (H) which is given as

Mmax(H) = 4Log H + 1.8 (16)

The corresponding feasibilities in (5), (6), (9) and (16) could indicate possible association and characterization of the most likely source of the given earthquake population in each seismogenic source zone.

Earthquakes are not equally distributed in space-time, although probably the seismic events follow physical causalities which are not fully known. Therefore, at least the strongest earthquakes can be assumed to be independent random events. Considering the probability of occurrence of these seismic events in a time interval (t), and assuming the Poisson process as the appropriate probability function applicable in the source zones, then the probability of occurrence (Pr) of an event with return time (Tmax) is given as

Pr = 1-exp(-t/Tmax) (17)

Because there were different constraints encountered in the correlation processes such as scarcity of seismic data and inadequate information concerning fault parameters. It became necessary to refer to (17) as an additional data and basis in the decision processes. The time interval is assumed to be 100 years. Slemmons (1981) had described a characterization scheme for fault rate activity. The classification is as follows: (a) fault not active; (b) hardly active; (c) well developed geomorphologically (medium to high); (d) high; (e) very high; and (f) extremely

high. The basis of the classification was the inverse of the linear slip rate as the constant slope of a linear relation between recurrence time and dislocation (eq.14) which is expressed in terms of magnitude. For slip rate of 10 cm/yr, the fault rate of activity is extremely high for magnitude range 4.8-9, for slip rate of 1 cm/yr, the fault rate activity varies from extremely high to very high for the magnitude range 4.7-9, for slip rate 0.1 cm/yr, the fault rate activity also varies from extremely high-to very high- to high for the magnitude range 4.7-9, for slip rate 0.01 cm/yr, the fault rate activity varies from very high- to high- to medium high for the magnitude range 4.7-9, and for slip rate 0.001 cm /yr, the fault rate activity varies from high-to medium high-to hardly active - to fault not active for the magnitude ranges 4.7 to 9.

Zone 14 (Sirhan-Turayf-Widyan Basins)

Tectonic Setting

The tectonic units composing Zone 14 are: Harrat al Harrah, Umm Wuai graben, Wadi as Sirhan and At Tawil faults, Sirhan At Turayf and Widyan basins. During the late Triassic to early Jurassic, rifting occurred at the northern end of the Arabian plate. A new Neo-Tethys was created. A north trending seaway developed which is possibly a successor of the Paleozoic Widyan basin. In the late to middle Jurassic, a limited Palmyrid-trend rifting occurred and the extrusion of the Devora volcanics was concurrent with the tectonic activity. During the late Jurassic, the Levant region also shows uplift and rifting coincident with massive Tayasir volcanism that could be responsible for the formation of Harrat al Harah. Early Senonian uplift and inversion of older structures in the Levant caused deformations along the Syrian arc and the onset of faulting in the Azraq Graben in Jordan with possible extension in northern portion of Saudi Arabia. A major basin evolved into the Azraq graben, a part of which could be the Sirhan at Turayf basin.

Seismicity

Historical data shows that there is one event of magnitude 5 located at coordinates 32N, 36E, and another one of magnitude 4 at 30N, 42.5E. The locations of these events seem to indicate that the first is generated by the Dead Sea transform fault, while the latter is within the vicinity of the Widyan basin.

Epicentral locations of instrumental data show that most of these are concentrated on Harrat al Harrah. However, the magnitude ranges of these events are from 2.5-3.8. The other events are scattered within the vicinity of Sirhan-Turayf and Widyan basins, and Wadi as Sirhan and At Tawil faults. The maximum magnitude of 5.4 in March 31, 1989 was observed to have occurred at Harrat al Harrah which could probably be due to fractures within the lava field.

Statistical analysis of the instrumental data using the cumulative frequency-magnitude relation

show that the seismicity parameters have respective values as follow: a = 3.13: b = -0.58; Mmax = 5.3. The historical data is insufficient for statistical treatment. A brief summary and description for the seismotectonic correlation for this seismogenic source zone is shown below.

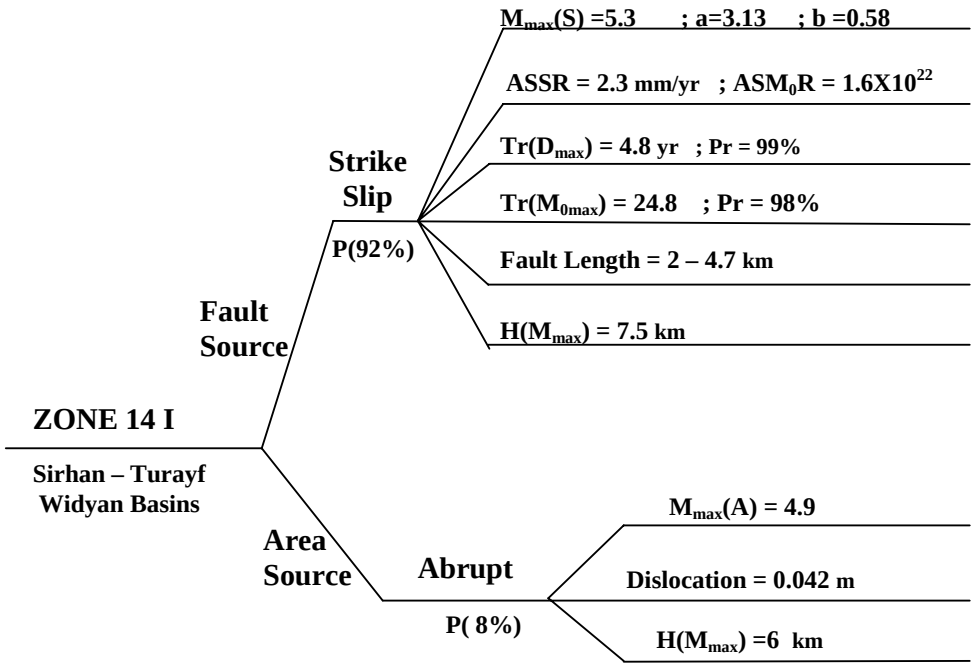

Zone 15 (Najd Fault Zone)

Tectonic Setting

The major tectonic component of Zone 15 is the Najd fault system. The north, northeast, and northwest trending pattern of the faults, anticlines, and arches in central and eastern Saudi Arabia appears to have formed in two tectonic stages. These are the Precambrian Amar Collision between 640-620 million years ago (Ma), followed by the development of the Najd Rift System between about 570-530 Ma (Stoeser & Camp 1985). The Amar collision was between the Afif and Ar Rayn terrane. The collision took place along the north trending Al Amar Idsas Suture bounded approximately from 22-25 degrees north and 43-45 degrees east whose longitudinal extension could be up to 29 degrees north based from aeromagnetic map and possibly as far as the Zagros suture (Johnson & Stewart 1994). The Afif terrane formed the eastern edge of a series of terranes (Midyan, Hijaz, Asir), while the Rayn micro-plate corresponds to central and eastern Arabia and is bounded to the west by the Al-Amar island arc. Following the Amar collision, the entire Arabian-Nubian Shield appears to have started collapsing in extension. The extensional collapse culminated in the development of the regionally extensive Najd Fault System and its complimentary rift basins that make up the Najd Rift System.

The sinistral Najd fault system consists of three main parallel fault zones, each about 5-10 km wide, that dislocated the much older (680-640 Ma) Nabitah Suture by approximately 250-300 km (Brown & Jackson 1960, Brown 1972, Moore 1979, Brown et al 1989). The fault system has a width of about 300 km and an exposed length of 1,100 km. The dislocation on the Najd west (Ruwah, Ad Dafinah, Nabitah), central (Ar Rika), and east (Halaban-Zarghat) faults are about 120-150 km, 80-100 km, and 50 km respectively. The fault movement was brittle and the plate motion along the faults was kinematic (Moore 1979, Howland 1979). In the subsurface, the Najd fault system extends across the western Rub Al Khali basin as interpreted from seismic, gravity and magnetic data. Pull-apart basins that align with the Najd fault system show syn-rift layered seismic reflections and salt structures (Dyer & Al-Husseini 1991, Faqira & Al-Hauwaj 1998).

Seismicity

No historical seismic events were observed to have occurred in this zone, and only 5 instrumental earthquakes were compiled. The observed maximum magnitude was 4.4 which had occurred in Nov. 6, 1997 in the vicinity of Kirsh gneiss and Ar Rika fault zone. The second event of lesser magnitude has a value of 4, occurring in Aug. 17, 1997 also within the vicinity of the Ar Rika fault zone. Since there are only 5 seismic events, the Utsu-Aki maximum likelihood was utilized in the evaluation of the values of the seismicity parameters. The obtained values of the seismic parameters are: a = 3.69; b = -0.74; Mmax = 4. However, the estimated maximum magnitude from the seismicity parameters may not be the appropriate value should dynamic dislocations from the 3 faults in this zone occur. Assuming an average fault length of 166 km, the equivalent magnitude for this fault length is 8.0 as obtained from equation (1).

A brief summary of the seismotectonic correlation for this zone is shown graphically by the accompanying logic tree diagram.

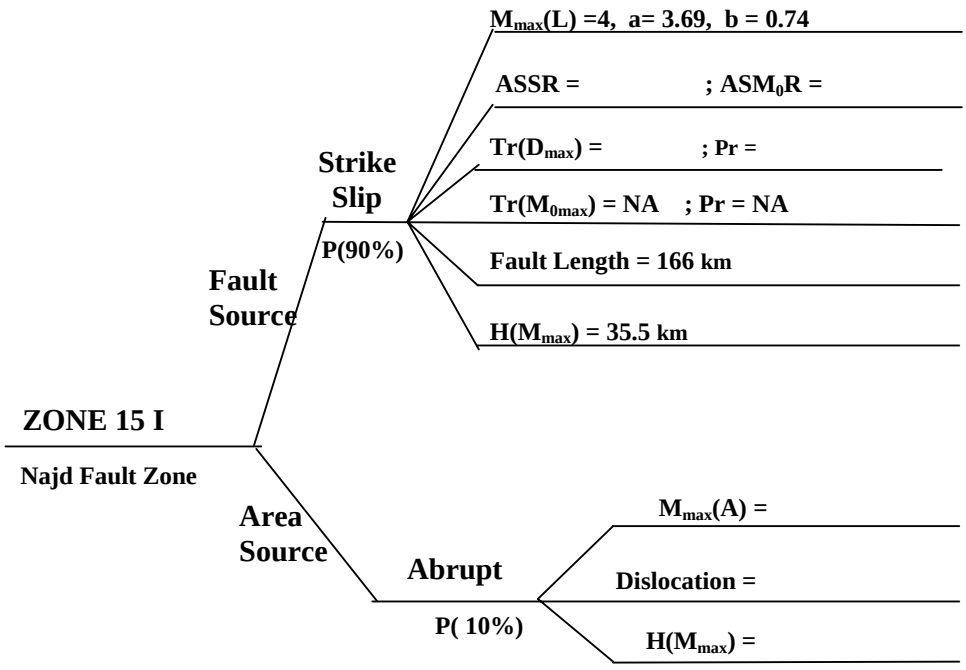

Zone 16 (Central Arabian Graben Zone)

Tectonic Setting

Zone 16 is roughly composed of the central Arabian graben and trough system; Wadi Batin and Abu Jifan fault; Summan platform, Khurais- Burgan and En Nala-Ghawar anticlines, Qatar Arch, and the Kuwait complex structures ranging from megascale, mesoscale, and microscale. The approximately 560 km compound graben system defines an arc concave to the northeast. It comprises six (6) major grabens and three (3) large synclinal troughs, together with subsidiary grabens and troughs. The major grabens are Majma, Al Barrah, Qaradan, Durma, Awsat, and Nisah. The Durma, Awsat, and Nisah lie entirely within the present region, which also includes 4 km of the eastern end of the Qaradan graben. The Majma, Awsat and Nisah grabens are compound structures. The Majma graben comprises many offset segments, whereas, the Awsat and Nisah grabens each consists of two overlapping segments. The three (3) large troughs are Buayja, Mughrah, and Sahba. Graben boundaries are defined high-angle normal faults commonly cutting the steep limbs of associated inward-facing monoclinal flexure zones. Trough margins are defined by inward-facing monoclinal flexures locally accompanied by subsidiary normal faults. Many grabens die out laterally through monoclinal flexures of decreasing amplitudes.

On the basis of stratigraphic and facies relationships, Powers et al. (1966) proposed that faulting on the central Arabian graben and trough system began in the Late-Cretaceous time and may have continued until the Eocene. The grabens developed between Late Cretaceous and the Late Quaternary, most movement being Paleogene age but succeeded by subsidiary Neogene and Quaternary movements.

Three (3) west-facing escarpments arranged in concentric arcs concave to the west dominate the topography. The western and highest escarpment, Jabal Tuwayq, is a double scarp. The western end is capped by the Tuwayq Mountain Limestone and the eastern end is capped by the Jubaila Limestone. The eastern end is the Jubayl escarpment capped of the Sulaiy Formation. The Durma basin lies west of the Tuwayq escarpment and the Kharj basin is situated between the Tuwayq and Al Jubayl escarpments.

The approximately 140 km Majma graben complex comprises many overlapping faults and en-echelon grabens replacing one another. The first is to the west and then to the east as the structure is traced from south to north (Powers et al 1966).The southern segment trends 340 degrees, while the northern segment trends 356 degrees. Displacement on their boundary faults range from 150-200 m. From south to north , the graben complex cuts outcrops from the

Dhruma formation to the Aruma formation. The 23 km Al Barrah graben trends 305 degrees. Displacements on its boundary faults are estimated to range from 200 – 300 m (Powers et al 1966). The graben is expressed by a relatively low dissected ridge that mainly exposes the Tuwayq Mountain limestone. The approximate length of the Durma-Nisah segment of the central Arabian graben system is 150 km and its width is about 25 km. The Nisah, Awsat, Durma, and Qaradan grabens are arranged en echelon. The Awsat and Nisah grabens are compound, each comprises two overlapping segment, the sense of overlap being the opposite of that displayed by the four grabens. Fault zones along graben margins commonly comprise a principal boundary fault, subsidiary antithetic or synthetic normal faults, and minor antithetic or synthetic extension faults, that is, small faults that result in layer-parallel elongation (Norris 1958).

The Qaradan graben is at least 12 km long and an average of 2.5 km width. The graben trends 310 degrees and its displacement on its boundary faults exceeds 400 m in the northeast. According to Powers et al (1966), the Qaradan graben is separated from the Durma graben by transverse fault striking 290 degrees. The exposed length of the Durma graben is about 63 km. Its width is from 1-1.5 km. It trends 295 degrees. Displacements on the boundary fault increases progressively westward. A few meters at the eastern end of the graben to about 100 m near longitude 46 degrees 27 minute east, 330 m near longitude 46 degrees and 17 minutes east, and about 400 m at the western end of the graben (Al Khadi & Hankock 1980). The Awsat graben can be traced for about 90 km. It comprises two segments each 1-2 km wide. Powers et al (1966) recorded an overlap of about 7 km, while present mapping shows the overlap of the graben boundary faults is about 25 km. The eastern segment lies north of the western segment Displacement on the high angle normal boundary faults are about 20-30 m close to the extreme western end of the structure, 200 m near (46 degrees, 8 minutes east), 300 m in the central section (46 degrees, 33 minutes east), and decline to about 50 m at the eastern end.

The Nisah graben is about 95 km in length and comprises two segments overlapping around 4 km along a common boundary fault near 46 degrees, 36 minutes east. The 1.5-2.5 km wide western sement trends 290 degrees at it western end and 280 degrees at its eastern end. The eastern segment which is 2.5-3.5 km wide trends 275 degrees. The Buayja trough is approximately 40 km in length. In the west, it is about 1 km wide and broadens to about 3 km in the east. Along most of its length, the trough forms a shallow topographic depression crossed by transverse wadis. The Mughrah trough is about 40 km long to the east from 47 degrees and 19 minutes east. It has a gentler fold than the Buayja trough. The structural homolog of the Nisah graben east of longitude 47 degrees and 10 minutes east is the Sahba trough. It has a broad

structural and topographic depression of about 8 km wide. According to Brown (1972), it is possible that this structure extends further east up to the Arabian Gulf.

Seismicity

Seismicity of the area has been studied mainly on the data from the Seismic Studies Center (SSC) of King Saud University, the Bahrain Seismic Network (BSN), the Qatar Seismic Network (QSN), the Kuwait National Seismic Network (KNSN), and Ambraseys (1988) compilation. Historical data indicates that an earthquake of magnitude 5.8 - 6.0 was reported to have occurred in 1832 near the Al-Ghawar reservoir and Qatar arch. Instrumental data show that the Al-Ghawar area and its vicinity has experienced 86 earthquakes (2.5<Md<5.4) from 1965-1998. Most of these seismic events are located south to southeast of the Ghawar reservoir and the rest on the west of Qatar peninsula. Clusters of seismic events were also to occur in the Qassim area. Range of magnitude of these events is from 3 to 3.8. Instrumental seismicity indicates that an observed maximum magnitude of 5.3 has occurred in the vicinity of the central anticlines of the Arabian platform in June 1, 2002.

The seismicity of Kuwait reveals two main cluster of events. The first is around the Minagish-Umm Gudair oil field zone, and the second is around the Raudhatain-Sabriya oil field. The spatial correlation of earthquakes and oil fields suggest that the seismic events have been induced by oil production. The historical seismicity in this area indicates a magnitude 5.5 occurring north of Kuwait in Sept. 9, 1903.

The historical data for this zone shows insufficiency for the determination of seismicity parameters, while from the instrumental data the values of the seismicity parameters are as follows: a = 3.54; b = -0.64; and Mmax = 5.4

A brief summary and description of the seismotectonic correlation for this zone is graphically presented along with logic tree diagram.

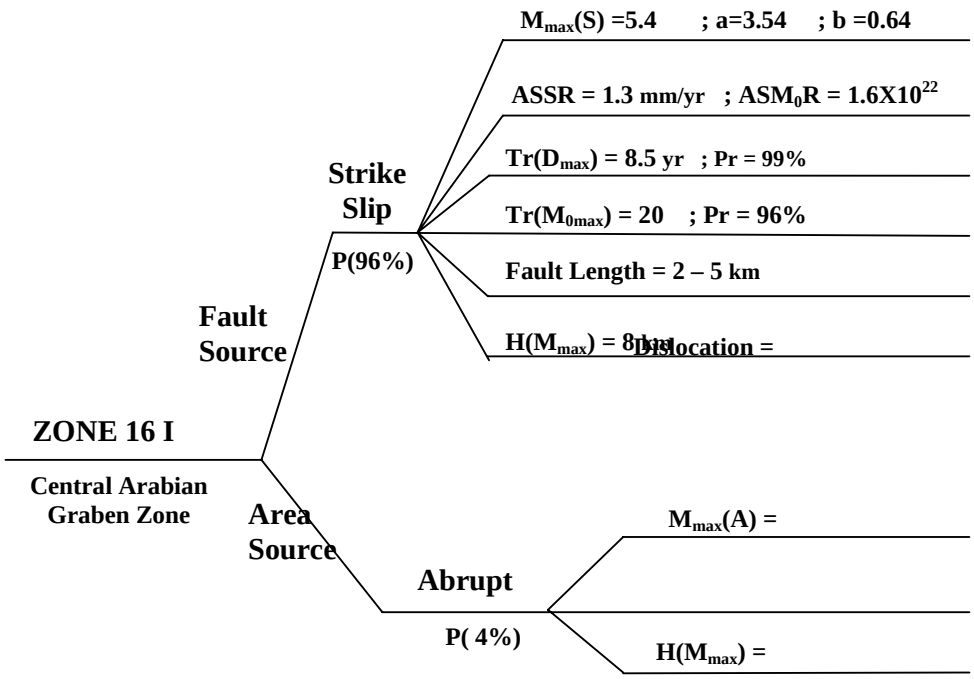

Zone 17 (Arabian Gulf)

Tectonic Setting

During the early to late middle Jurassic, the north trending Gotnia basin became established across the head of the Arabian gulf possibly separated by the Rimthan arch from its southern extension, the Arabian basin. The Gotnia basin allowed direct access for the open Neo-Tethys far across the Arabian platform. In the middle Jurassic, incipient graben system with a northwesterly trend developed at the southern margin of the Arabian plate. They began as a terrestrial to continental infill of erosional lows or pre-rift structural depressions, and culminated as rift troughs containing shallow water carbonates in the middle Jurassic. At the beginning of the Cretaceous, global sea level was relatively high, and the remnant of the Gotnia basin underwent rapid subsidence in the eastern part. At the time of high sea level, a shallow epeiric sea inundated the eastern platform of the Arabian plate. During the late Paleocene to early Oligocene, the Hercynian structural trends of the central Arabian arch continued to modify the morphology of the foreland basins. This became progressively narrower as it was filled in, until it became structurally neutralized. During the Pleistocene, sea level was low, and east of the Arabian arch, the shallow epicontinental Arabian gulf began to take its present shape (Ziegler 2001).

Seismicity

The spatial distribution of epicenters shows a scattered location of earthquake events, except along the common boundary that separate Zones 17 and 18, where a thin line of NW trending

concentration can be seen. The scattering seems to be distributed all over the basin. Some are located in the Zagros fold belt area that belongs to this zone. The Arabian gulf seismic zone is both historically and instrumentally active. A maximum magnitude of 5.9 is observed to have occurred in Aug. 16, 1883 in the Zagros fold belt that belongs to the zone. A lesser event of magnitude 5.8 in March 6, 1956 was located in the basin. Instrumental data indicates that two earthquakes occurring in Nov. 7 1969 and in Sept 13, 2000 with the same magnitude value of 5 have occurred in the Zagros folded belt of the zone.

Statistical analysis was conducted for the two period of observation separately using the cumulative frequency-magnitude relation due to sufficiency of seismic data. The obtained values for the seismicity parameters from the historical data were: a = 4.15; b = -0.63; Mmax = 6.6; while for the instrumental data gives: a = 3.12; b = -0.55; Mmax = 5.6. A brief summary of the seismotectonic correlation for this source area is graphically provided by the accompanying logic tree diagram.

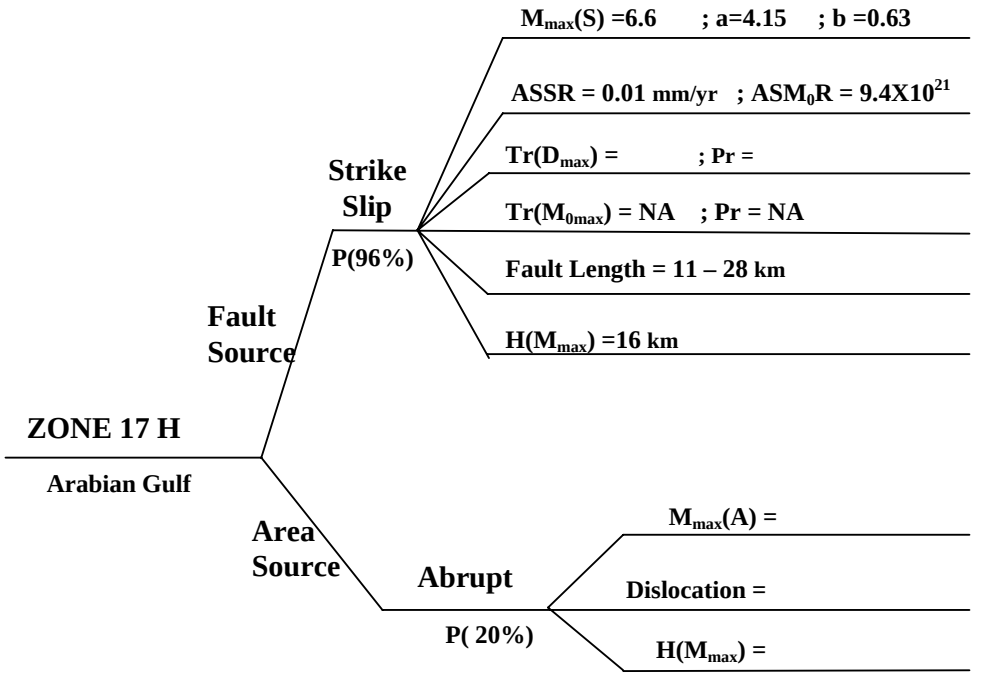

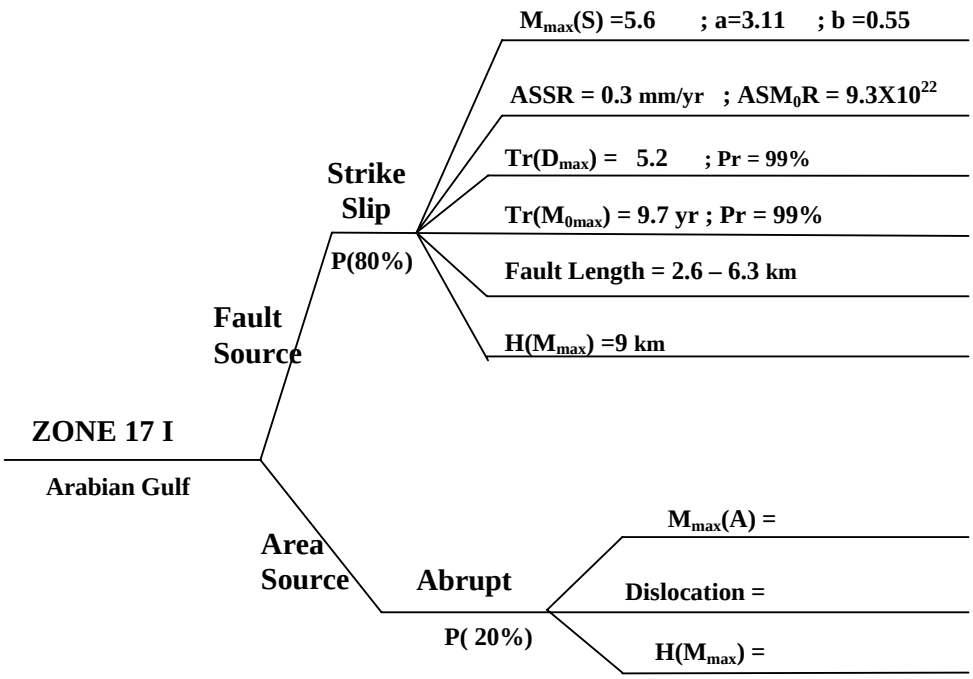

Zone 18 (Zagros Fold Zone)

Tectonic Setting

The primary tectonic unit in this source area is the folded zone of the Zagros Mountains. The Zagros Mountains are a broad belt of NW-SE folded and faulted Paleozoic, Mesozoic, and Cenozoic rocks with orogenic movements occurring in Late Tertiary. Zagros mountain foreland is composed of gentle folded rocks, elongated, parallel and contemporaneous structure to the belt. The continued convergence of the Afro-Arabian plate relative to the Iranian blocks is partially accommodated by folding of the Zagros sedimentary cover and by high angle reverse faulting of the underlying Precambrian Arabian basement. The sedimentary cover is decoupled from the basement by the thick Infra-Cambrian Hormuz salt bed which acts as a detachment surface. The synchronous widespread deformation of the sedimentary cover and the basement is a unique feature for the Zagros region. The present basement faulting beneath the Zagros fold belt as due to re-activation of pre-existing normal faults as reverse faults in the Arabian continental margin is in conformity with assumption. Crustal models constrained by Bouger gravity anomalies indicate a dipping Moho about 1 degree to the northeast and increases to about 5 degrees near the Main Zagros Thrust (MZT). The Moho depth increases from 40 km beneath the leading edge of the foreland basins (Mesopotamian Deep and Arabian Gulf) to 65 km beneath the MZT (Barazangi 1986).

Seismicity

The entire Zagros folded belt is the most active seismic area in this seismogenic source zone. The folded zone is characterized by both shallow and non-shallow earthquakes. The earthquakes locations in this folded belt define a zone of about 200 km wide that runs parallel to its central axis. Most of the earthquakes are crustal seismic events that occur in the portion of the Arabian plate.

This seismogenic source zone is historically and recently active. Its historical data indicates that an earthquake of magnitude 5.7 has occurred in March 21 1875. One 5.5 magnitude in Feb 4, 1934, and 3 magnitude 5.4 in 1925, 1939, and 1958 have occurred in this source zone. In 1972, a magnitude 6.1 has occurred which was followed by a magnitude 6 in 1976 in a span of 4 years. A survey of the range of magnitude in this zone is seen to be frequented many times with magnitude 5 and above.

Statistical analysis of the compiled seismic data using the cumulative frequency-magnitude relation gives values for the seismicity parameters for the historical period as: a = 6.11; b = -0.9; Mmax = 6.8; and for the instrumental data gives for a = 6.28; b = -0.96; Mmax = 6.6.

A brief description and summary of the seismotectonic correlation for this zone is shown below.

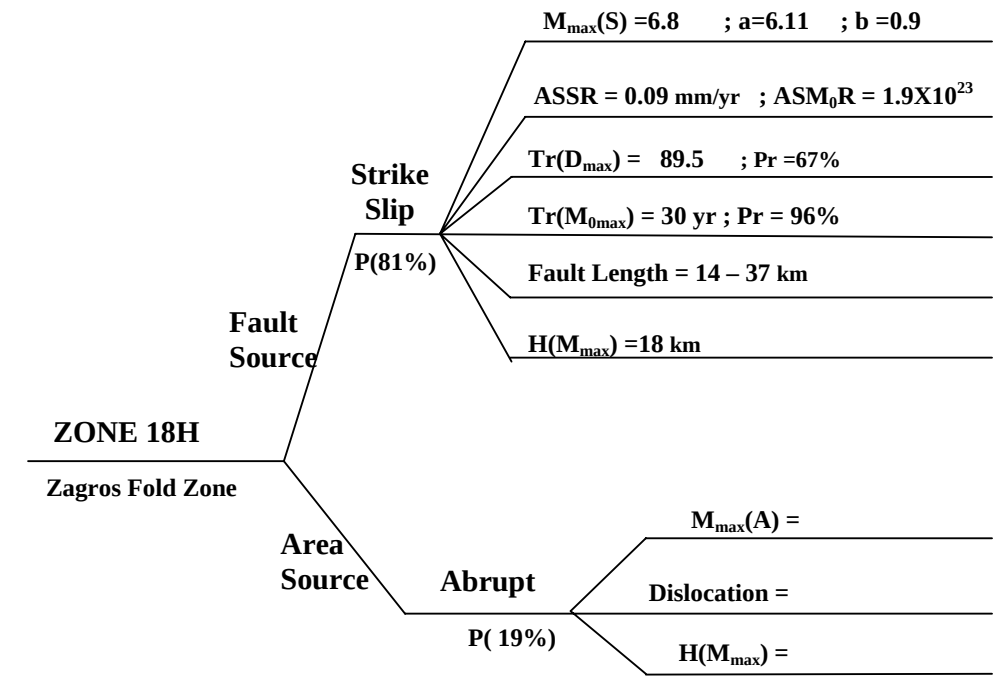

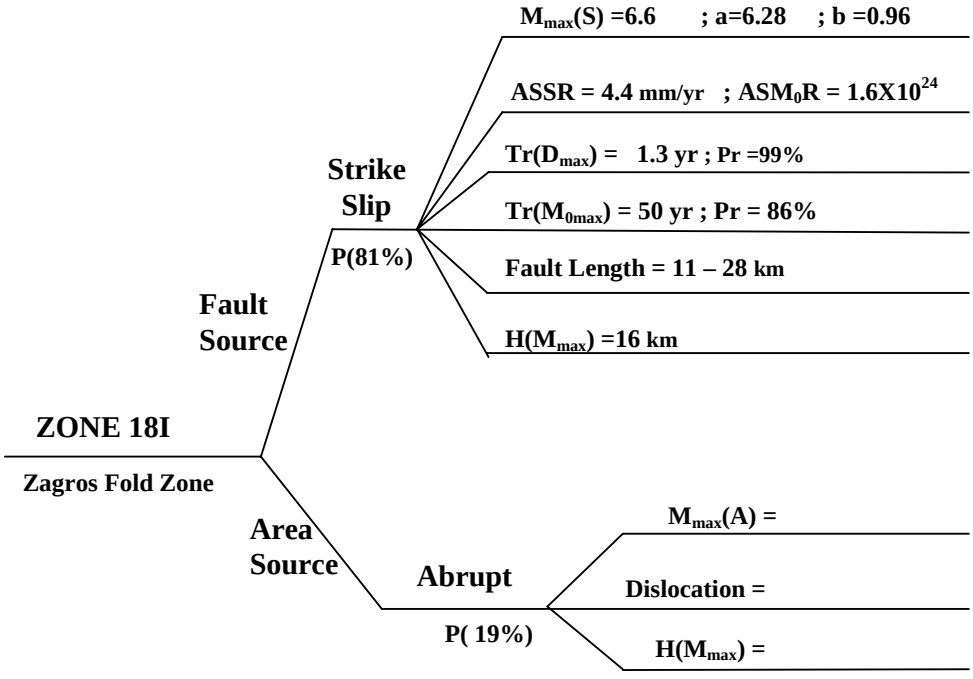

Zone 19 (Sanadaj-Sirjan Ranges)

Tectonic Setting

The main Zagros thrust with its crush zone and the Sanandaj-Sirjan ranges are the principal tectonic units in this seismogenic zone. From the late middle Eocene to early Miocene, the Arabian plate began to impact southern Asia, and the Zagros oregeny began. In the late Permian, continental rifting and spreading took place along the present day Zagros suture as the Neo-Tethys ocean started to form. The former intra-shelf basins, Lurestan and Khuzestan in Iran have been consolidated to form one long relatively narrow foredeep trough along the Zagros fold belt. Close to the Zagros main thrust (MZT) silt and sandstones were deposited in the foredeep. Ophiolite nappes were emplaced along the MZT. During the Miocene, strong compression occurred as Arabia was driven into Eurasia. On the eastern flank of the Arabian plate, the thrusting of the Sanandaj-Sirjan zone onto the plate is evidence of the continental collision. As continent to continent collision continued, the Zagros oregeny intensified and thrust and folds belts migrated southwestward to their position in the Gulf region. Phases of compression led to the formation and deformation of the Zagros foredeep in front of the Zagros mountain belt. The Zagros foredeep (Mesopotamian basin) roughly corresponds to the zone between the Mesozoic unstable shelf to the west and the limit of the Zagros fold belt to the east.

Seismicity

The seismicity of this seismogenic source zone is governed mainly by two tectonic sources. These are the effects of underthrusting of the MZT by the Arabian plate and the convergence zone of southern Iran and Oman. However, the spatial distribution of earthquake epicenters in the MZT and the Sanandaj-Sirhan ranges is not as concentrated as the distribution in the Zagros folded belt and the convergence zone. Historically and recently this source area is seismically active. In May 2, 1963, a strong earthquake of magnitude 5.9 has occurred in the location of the MZT. From the historical data, it is seen that many seismic events of magnitude 5 and above have frequented this source area. In June 21, 1965 and in April 12, 1971 earthquakes of magnitude 6 have occurred. These two earthquakes are located near each other in the vicinity of the MZT and collision zone. It is also noted, that this period is frequented with seismic events whose magnitude values are 5 and above. Statistical analysis conducted for the historical and instrumental data using the cumulative frequency-magnitude relation gives the following seismicity parameters values for a = 5.06; b = -0.79; Mmax = 6.4 of the historical data, and a = 6.28; b = -0.96; Mmax = 6.8 for the instrumental data. A brief summary of the seismotectonic correlation for this seismic zone is graphically shown below.

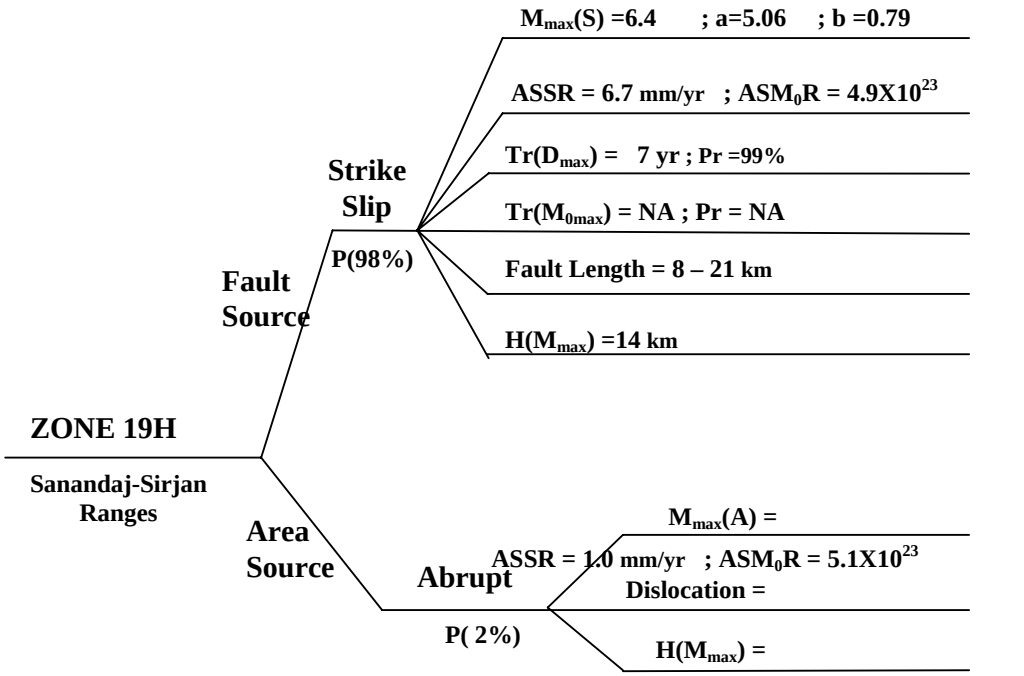

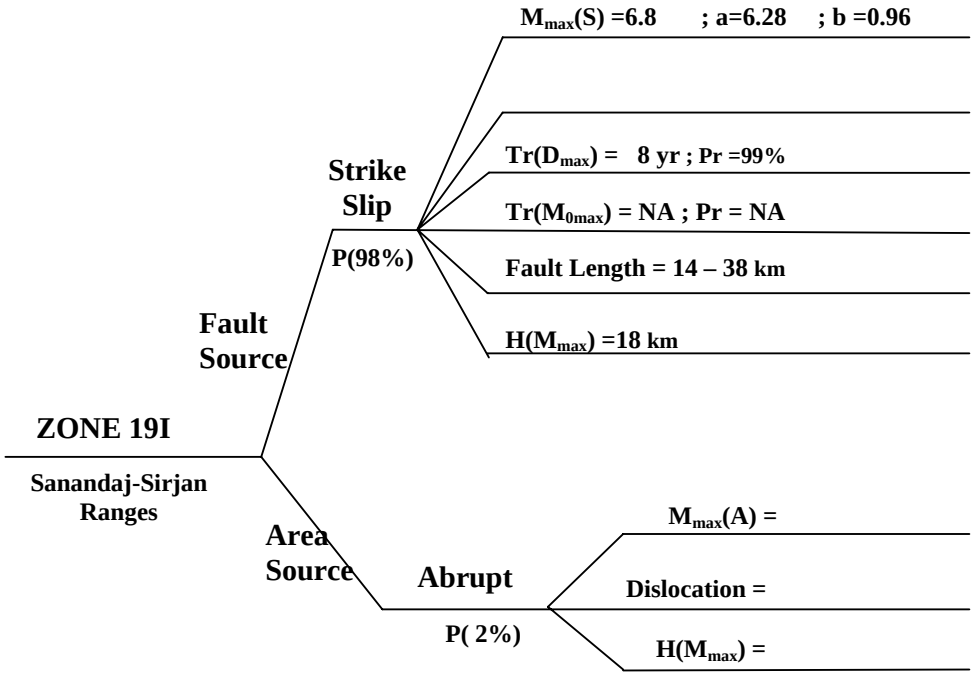

Zone 20 (Eastern Yemen)

Tectonic Setting

The Marib-Shabwa basin is a west northwest-east southeast trending late Jurassic rift system which lies in southwestern Yemen. The orientation of the system corresponds to the Najd trend which probably exerted some control on the orientation of the Jurassic rift. It is part of an extensive system of basins which trend across southern Arabia and the Horn of Africa. To the east, the system extends almost to the island of Socotra. The structural framework of the Marib-Shabwa basin was established in Kimmeridgian-Tithonian times when the major period of rifting occurred. The rift widens considerably in the Shabwa area, and an important north-south (Hadramaut Trend) lineaments, such as the Shabwa arch and the Ayadin fault are present. This trend may be inherited from an underlying Proterozoic arc terrane suture. The Marib-Shabwa basin can be subdivided into several linked grabens and half-grabens. Basin geometry exercised a profound control on sedimentation by the central Marib-Shabwa basin both during syn-rit and post rift times. During syn-rift times, the deep half-grabens on the basin margin and adjacent to the Central High trapped clastics in their axes and starved the central basinal areas. During post-rift times, the block-faulted topography controlled the direction of salt migration, with salt forming linear ridges overlying footwall highs. As a result, post-rift sedimentation was concentrated in a series of linear salt-withdrawal basins, overlying syn-rift lows.

Seismicity

Only two seismic events are recorded in this seismogenic source zone. One is historical and the other is instrumental. The historical event has a magnitude of 4.8 occurring in June 21, 1916 whose location is in the Hadramaut arches of eastern Yemen, while the instrumental data has occurred in July 21, 1997 and located also in the vicinity of the arches. No statistical analysis is performed for this seismogenic source zone, but a brief summary of the seismotectonic correlation is presented in the accompanying graphical presentation of a logic tree diagram.

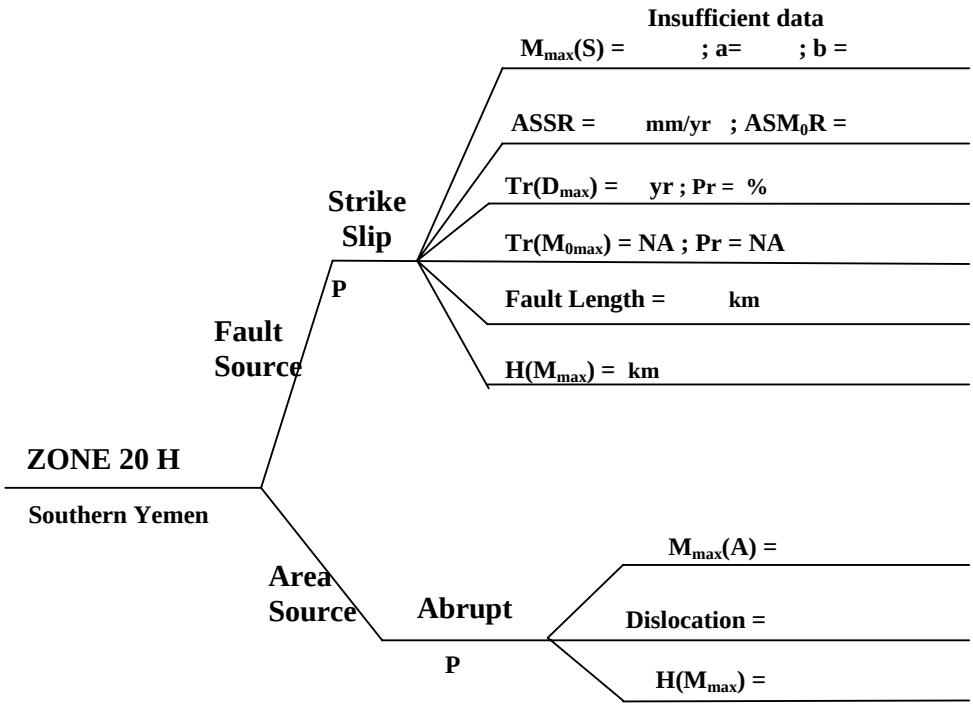

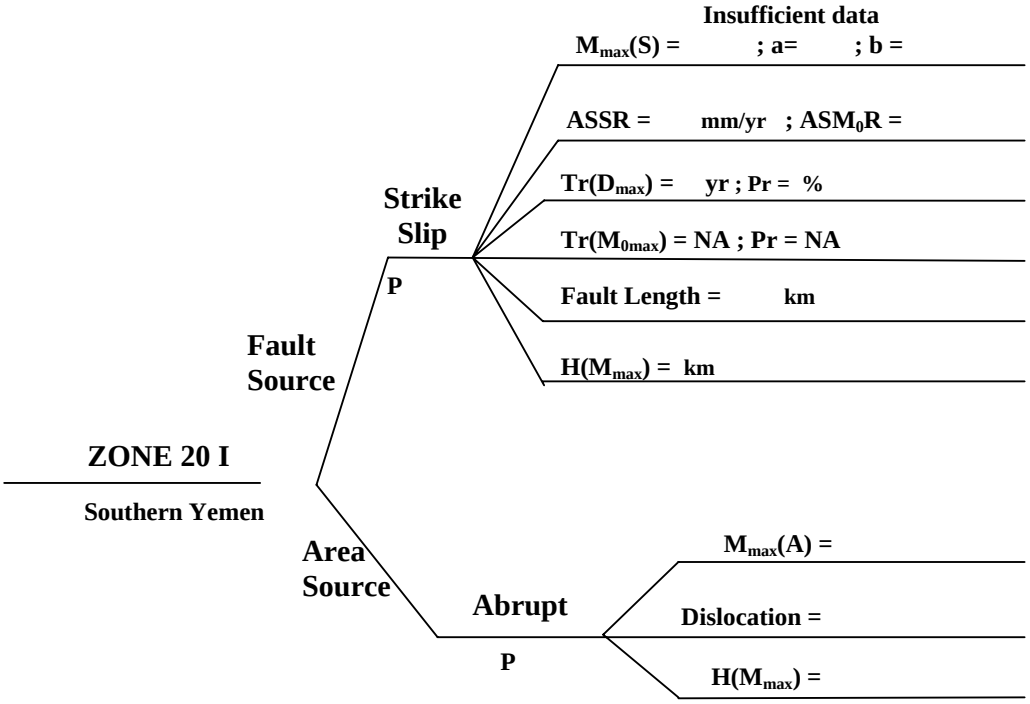

Zone 21 (Rub Al Khali-Ghudun Basins)

Tectonic Setting

The most important tectonic elements in Oman are the three known Infracambrian salt basins. These are the Fahud and Ghaba salt basins in the north and the south Oman salt basin. Immediately to the west of the south Oman basin is the Ghudun-Khasfah high. It shows a north trending positive linear gravity anomaly that separates the south Oman basin from a gravity low to the west. It is thought that the western gravity low in the extreme southwest represents a fourth Infracambrian basin. This new basin is called Ghudun salt basin and appears to be comparable in areal extent with the Ghaba basin and analogous with the other Oman salt basins. The depth of the basement is estimated to be from 8-10 km.

The tectonic history of the Ghaba salt basin is dominated by compressional events ranging in age from late Precambrian to Tertiary. The Ghaba salt basin is described as a push-down basin. The loading of the Oman Mountains led to the development of foreland basins. Loading from the north resulted in a regional dip in that direction on which the Mesozoic carbonate section began to slide, resulting in a series of extensional faults of WNW oreintation. This event allowed reactivation of the salt and many diapirs developed.

Seismicity

There are only 8 documented seismic events in this seismogenic source zone. Two were historical and 6 are instrumental. The maximum magnitude observed for the historical is 5.6 in Aug 20, 1954 which is located the Rub Al khali basin. The observed maximum magnitude for the instrumental data is 5 in Aug 20, 1997 which is also located in the basin. Due to seismic data constraint, statistical analysis is conducted mainly with the instrumental period of observation using Utsu (1965) maximum likelihood estimate of the values of the seismicity parameters. These are: a = 6.78; b = -0.96; Mmax = 4.7. A brief summary of the seismotectonic correlation is graphically presented by the accompanying logic tree diagram.

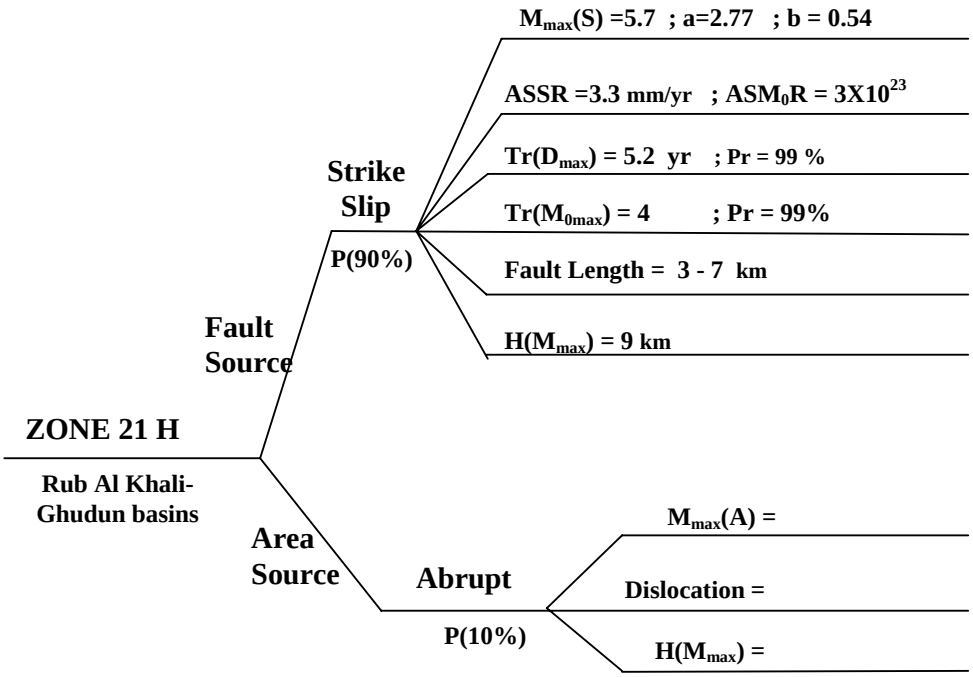

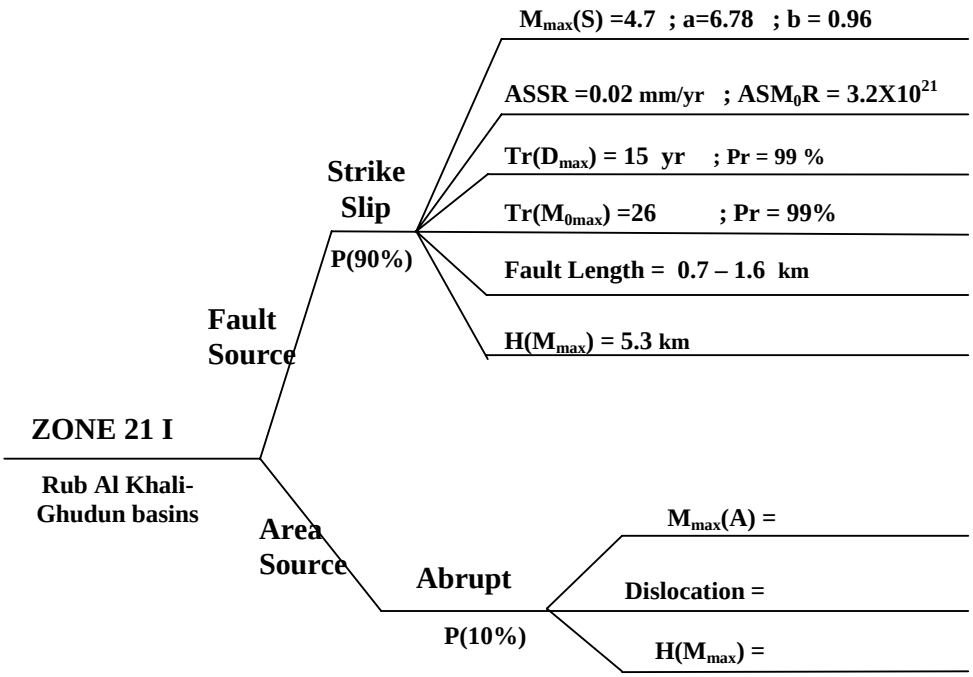

Zone 22 (Dibba-Bandar Abas Region)

Tectonic Setting

The primary tectonic units in this source zone are the Dibba fault and the Hormuz salt basin south of the Arabian gulf. The Dibba line in Oman marks a probable former transform fault. To its south, Cretaceous subduction began in Neo-Tethys 2, with back arc spreading leading to the development of what became the Semail Ophiolite nappe. Because of the very narrow microcontinent Jbel Qamar-Kawr ridge separating the Neo-Tethys 1 and 2, there was little effective resistance to the subduction process until the Maastrichian, when inability to consume the Oman sector of the Arabian continental process to a halt. With compressive stresses absorbed in Paleo-Tethys, late Cretaceous obduction in Neo-Tethys 1 and 2 did not lead to creation of the Oman and Zagros mountains.

In central Arabia, there was a slow but progressive infill of the intrashelf basins through repetitive shoaling upward carbonate cycles in the late Jurassic. At the beginning of the Cretaceous, global sea level was high and consequently most of the Arabian plate accumulated almost exclusively shallow marine carbonates. The Arabian basin was rapidly infilled, first by carbonates and later bu terrigenous clastics. In the late early Cretaceous, extensive rudist banks colonized the shelf breaks to the intrashelf basins such as in the southern gulf. Following the opening of the Atlantic ocean, a distinct change in motion of the Arabian plate has been postulated by Al Fares et al (1998). Far field stresses have thought to have resulted in the uplift and erosion of the western part of the Arabian shield and the supply eastward of large amounts of terrigenous clastics and shallow marine sands. The plate stress, combined with sufficient sediment loading served to trigger the growth of salt structures in the area of the southern Arabian gulf over which numerous rudist banks developed. At the southern portion of the Arabian gulf is where the Hormuz salt basin lies. The Hormuz is interpreted as a syn-rift sequence. This interpretation implies that the Hormuz evaporate basins were intra-continental (Ziegler 2001).

Seismicity

Two lines of spatial distribution of epicenters can be distinguishingly seen in this seismogenic source zone. The first which is a thin line of distribution is along the Dibba fault in northern Oman. The second has a wider zone of epicenter distribution. It is the convergence zone between southwestern Iran and northwestern Oman, a line known as Oman line that passes west of the Lut block in Iran. This seismic source area is both historically and instrumentally active. Two earthquakes of magnitude 6.4 occurring in Jan 10, 1897 and the other in July 9, 1902 were

located in the convergence zone. Likewise, two earthquakes of magnitude 6.2 have also occurred in March 21, 1977 and Apr 1, 1977 in almost the same location. It is noted that this seismogenic source zone seems to have frequent earthquakes of above magnitude 6 and many seismic events above magnitude 5. Statistical analysis of the historical and instrumental data using the cumulative frequency-magnitude relation gives for the historical seismicity parameters the values for a = 4.67; b = 0.68; Mmax = 6.8; and for the instrumental data are: a = 4.98; b = 0.74; Mmax = 6.8. A brief summary of the seismotectonic correlation for this source zone is graphically presented with the accompanying logic tree diagram.

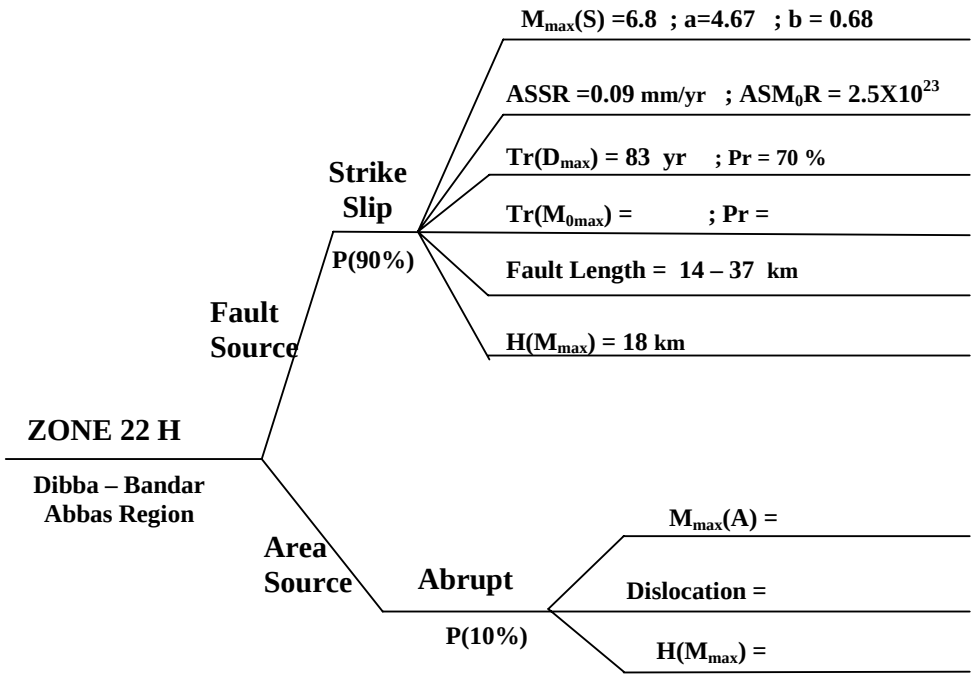

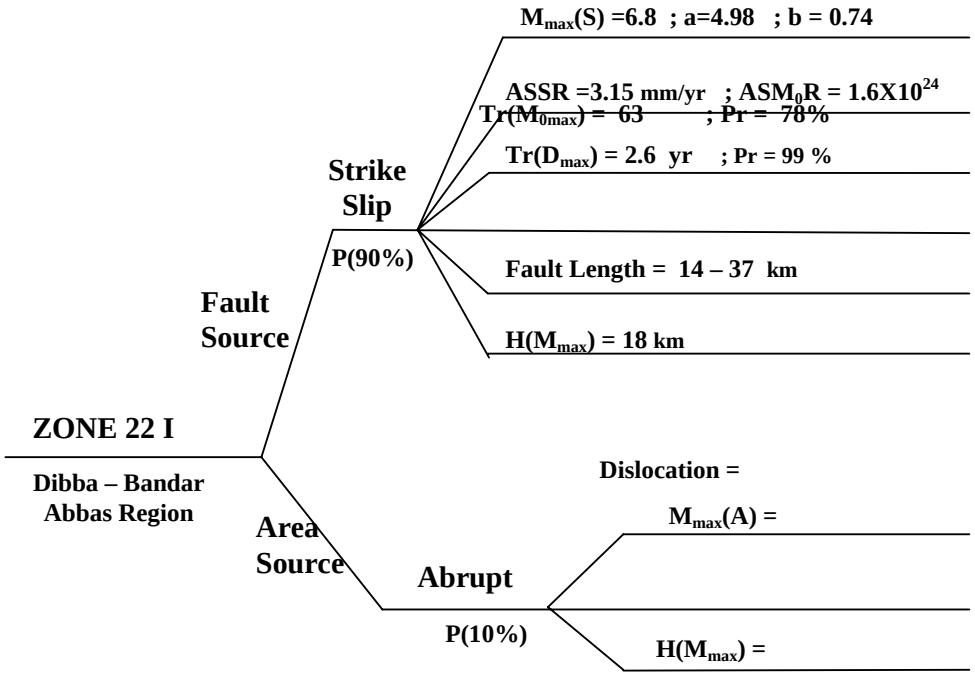

Zone 23 (Hawasina-Makran Thrust Region)

Tectonic Setting

During the rift cycle one (Vendian/Infracambrian period), a series N-S to NE-SW trending basement high in Oman may have developed. These are the Ghudun-Khasfah high, the Anzaus-Rudhwan ridge, and the Makarem-Mabrouk high separating different basin segments. The event is associated with igneous activity (Oman mountains) and is followed by a thermal subsidence phase. Around 110 Ma, the Atlantic ocean begins to open, leading to the closure of the Neo-Tethys between the Afro-Arabian and Eurasian plates. A northeasterly dipping intra-oceanic subduction zone develops, accompanied by arc-spreading. At 93 Ma, this subduction complex collided with the continental crust of Oman creating the Zagros-Makran subduction zone . The initial uplift has been described as a mobile or stationary fore-bulge that preceded downwarping of the foreland ahead of the advancing thrust front. The second rift cycle which is also a compressional event as in rift cycle one occurred in the late Eocene to Miocene time. This event was responsible for the folding and short distance thrusting of the of the allochthonous units of the upper Cretaceous and Tertiary neo-authochthonous cover cover in the foredeep basins. The Huwayyah anticline is a unique example. The Tertiary compressional event caused reactivation of the late Cretaceous basal ramp fault to form the Huwayyah anticline and associated thrust strike-slip faults. The second event can be correlated with the Zagros oregeny in Iran. Two angle reverse faults are found in the western flank of the Huwayyah anticline. These are oriented in a NNW and ENE directions parallel and perpendicular to the fold of the anticline respectively. The main reverse fault is named Auha. A second reverse fault lies east of Auha. These faults probably originated as ordinary west dipping thrust on the western flank of the anticline. The displacement of the strike-slip faults are in the order of a few several meters and the sense of displacement suggest dextral movement.

The northern flank of the Sohar basin is limited by the Makran accretionary prism. This is an elongated and structurally complex thrust belt resulting from the subduction of oceanic basement under the Eurasian plate. The Makran is actively today and advancing southward at a maximum rate of some 10 cm/yr. Large overthrust anticline are recognized along the frontal thrust belt. Towards the core of the accretionary prism fault density increases creating a highly complex and deformed thrust belt.

Seismicity

Spatial distribution of earthquake epicenters in this zone is sparse. Some are found to be located in the Zagros-Makran subduction zone, in the gulf of Oman, the Hawasina thrust sheets, and in the Maradi fault zone. One earthquake event for each in the Hawasina and Maradi fault is located. Historical seismicity indicates that the observed maximum magnitude is 5.5 in May 13, 1905 which is located in the gulf of Oman. The instrumentally observed maximum event has a magnitude of 4.8 in June 15, 1977 and likewise is located in the gulf area.

Seismicity analysis for the historical and instrumental data using the Utsu-Aki maximum likelihood estimate method gives the following values for the historical seismicity parameters: a = 3.8; b = -0.71; Mmax = 5.9, and for the instrumental data: a = 3.47; b = --0.76; Mmax = 4.8.

A brief summary for the seismotectonic correlation is presented with the logic tree diagram.

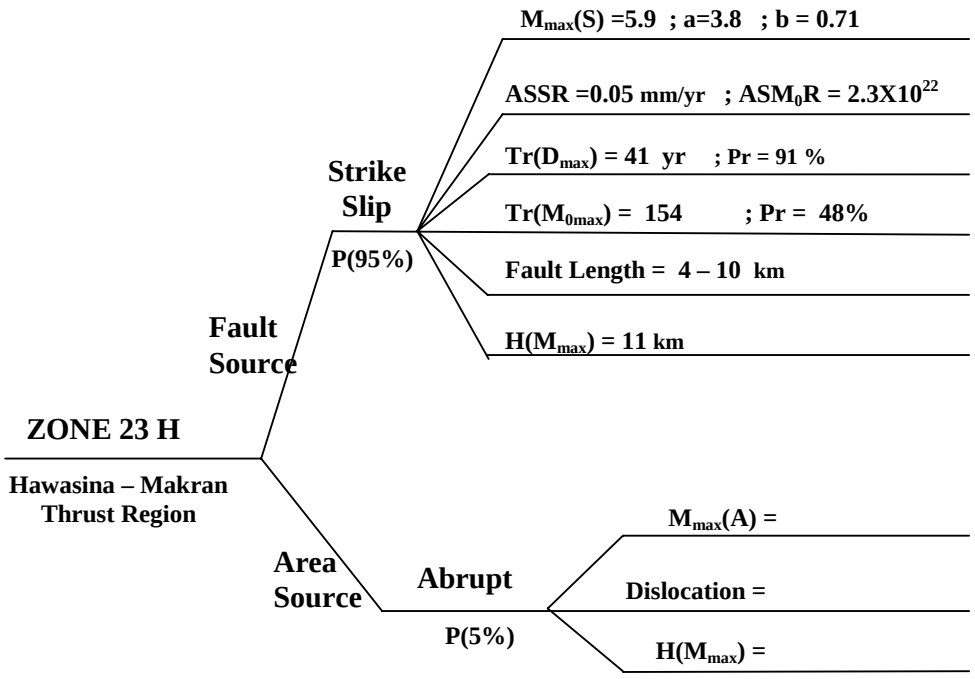

Zone 24 (East Sheba Ridge)

Tectonic Setting

In the late Campanian-early Mastrichian, a rift developed between Seychelles and India. This rifting culminated in the Deccan volcanic event at approximately 64 Ma, when a new oceanic spreading zone which is the Carlsberg ridge developed. Above the Carlsberg ridge to the northeast is another ridge which is called the East Sheba ridge that connects the main trough of the Gulf of Aden. The Sheba ridge is bounded by the Alula-Fartak trench to the west and by the Owen fracture zone to the east.

Seismicity

Epicenters distribution in this zone shows good correlation between seismicity and topography. The main line of epicenters follows the crest of the Carlsberg ridge that turns at 10.5N, 57.0E to a NNE direction, continuing in this orientation up to 13N. At this latitude, it turns abruptly in a northwestward direction. The line of epicenters lies closely along the axis of the Sheba ridge to about 56.5E where the seismic events are clustered.

This zone is active historically up to the present time. The observed maximum earthquake in the histrorical time has a magnitude of 6.6 in Aug 17, 1899. This event is located off the main ridge axis. The instrumental maximum magnitude is 5.6 in Dec 5, 1981. Its location is likewise in the vicinity of the main ridge.

Statistical analysis conducted on the historical and instrumental data using the cumulative frequency-magnitude relation gives for the values of the historical seismicity parameters as follow: a = 3.77; b= -0.52; Mmax = 7.3; while for the instrumental data analysis are obtained the values for a = 7.94; b = -1.35; Mmax = 5.9.

A brief summary of the seismotectonic activity for this zone is accompanied by its graphical presentation of the logic tree diagram.

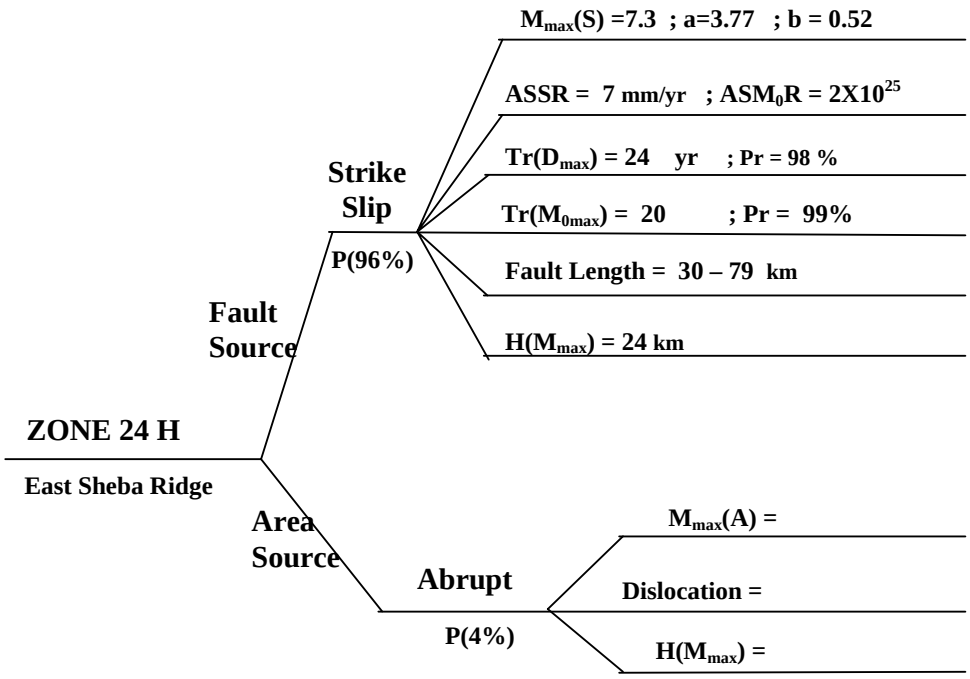

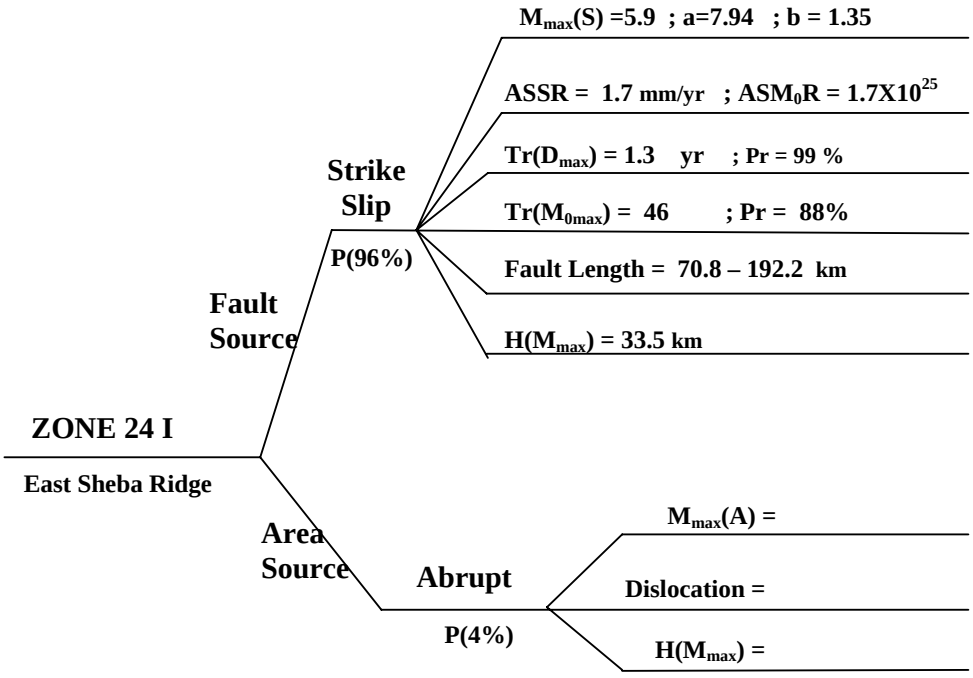

Zone 25 (Masirah Fault System)

Tectonic Setting

At the Cretaceous/Tertiary boundary, intra-oceanic north over south thrusting between the lower and upper ophiolitic nappes of Masirah island occurred. Along the east coast of Oman, largely offshore under Masirah bay and Sawqrah bay, a narrow gently folded foreland basin which is the Masirah trough was developed. The western margin is bounded by normal faults reactivating Mesozoic rift related faults. On its eastern margin, a wedge of ophiolitic and probably continental slope sediments is largely underthrusted below the eastern and uplifted part of the foredeep basin. To the south of the trough lies the Masirah transform fault.

Seismicity

The number of seismic events compiled for the historical and instrumental data are 7 and 4 respectively for this zone. The maximum historical event has a magnitude of 6.5 in Oct 10, 1900. Its epicenter is at 16N, 60E which is in the Owen fracture zone. For the instrumental data, the maximum magnitude is 5.2 in Mar 15, 1983. This event is also placed in the Owen transform fault. Only one event of magnitude 5.1 is found to occur in the Masirah thrust zone, while others can be considered as area source earthquakes or could be due to the influence of the Masirah and Owen transform faults.

Seismic parameters for this zone have been determined using the Utsu (1965) maximum likelihood estimate method for the historical and instrumental data. The values of the parameters are as follow: a = 7.55; b = -1.3; Mmax = 6.1 for the historical, and a = 3.64; b = -1.58; Mmax = 5.2 for the instrumental.

A brief summary of the seismotectonic activity for this zone is accompanied by the graphical presentation of the logic tree diagram.

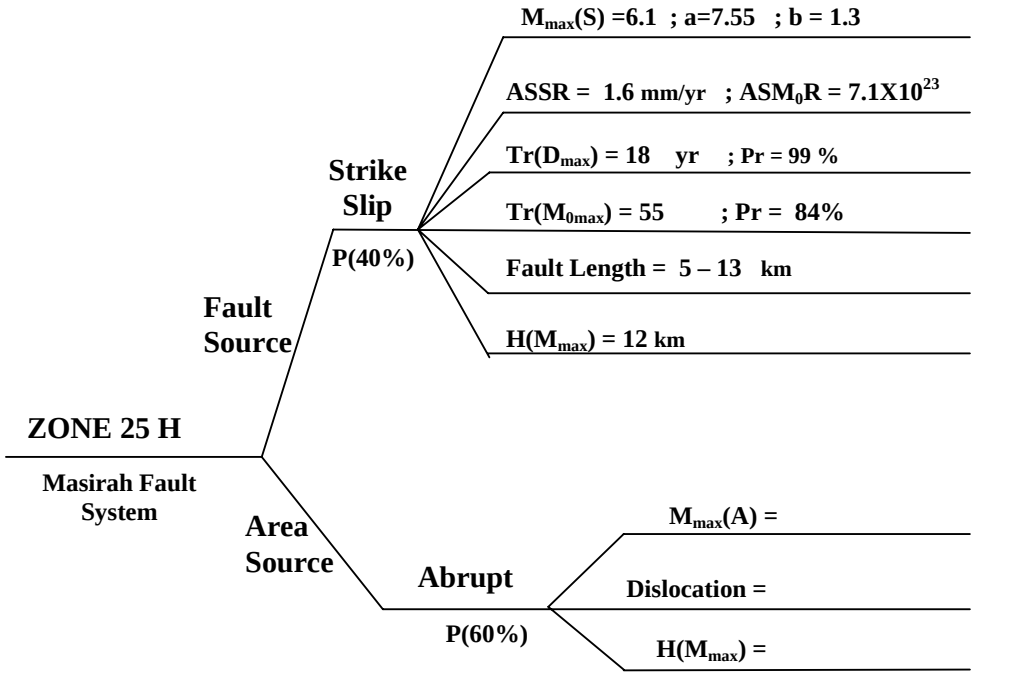

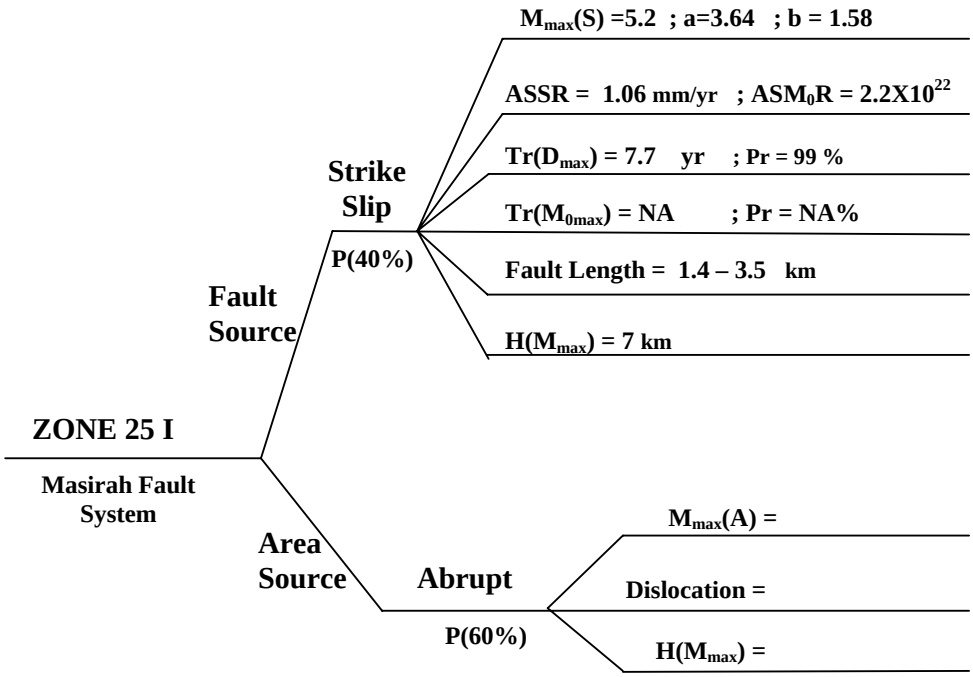

CHAPTER 4

DESIGN EARTHQUKE GROUND MOTION

Earthquake design load for a building is generally defined in building codes in term of design ground motion parameters estimated for the respected site. In the Saudi building Code, the design ground motion is defined by maximum considered earthquake spectral response accelerations at short period "S_s" & long period "S_1", which is consistent with IBC-03 (NEHRP 2000)". Mapped S_s and S_1 are furnished in this study based on probabilistic assessment of seismic hazard in the Kingdom considering the most recent local and regional seismicity and tectonic features. Basis of the probabilistic modeling which involves interrelated multidisciplinary geological, seismological, and seismotectonic studies of seismic sources and data are explained in the pervious chapters. Summary of the procedure and the computer modelling of estimation and mapping S_s and S_1 is given below.

4.1 Data Treatment

A counter-checking of all the relevant data entries in the catalogues was undertaken to ensure non-duplication of the same earthquake events. For the overlapping years of the seismic data, limiting and distinguishing procedures for the space-time distribution of the data were followed to avoid duplication. To consider two or more data points as one single event should have less than 25 seconds difference in their origin time in a location of 200 km. For repetitive events, the USGS data is given preference in the selection.

4.1.1 Reduction of Cluster Events from the Database

Three processes were followed roughly in the reduction of clusters in the database. An initial logarithmic cumulative frequency (LogN) versus magnitude (M) plot is prepared from the original data. Using the larger range of magnitude from the data as a guide, an eye fitted or tentative line is drawn through the plotted data points. By inspection of the graphs, deviations of the data points can be observed. From the observations, the deviations in reference to the larger range of magnitudes can be reduced. The deviations can also be visualized from a space-time window. The space-time window can be roughly estimated from Utsu-Seki and Omori aftershocks equations respectively to reduce the anomalous deviations. In this approximate process of removal, presence of clustering can only be reduced, but not entirely eliminated.

4.1.2 Completeness of Database

Incompleteness of database cannot be avoided as there several factors and constraints that are involved. Absence and insufficiency, and or low detection capability of sensing seismic instruments in microseismic observation of earthquakes. Scarcity and inadequacy of physical factors involved in the macroseismic observation of seismic events. Completeness analysis of the data base was not conducted due to encountered constraints that can hamper the analysis. These are the subdivision of the database in two period of observation, the observed insufficiency of seismic data in most of the seismogenic source zones, and in view of zero number of seismic events in some magnitude intervals.

4.1.3 Missing Magnitudes

Missing magnitudes from the historical up to the instrumental period were not considered. The magnitude interval characterizing the missing magnitude for the historical data is large (1.5-2 units) as deduced from Ambraseys (1988), while for the instrumental events are less than 3. The effects of the distribution and inclusion of these missing events shall be similar to the presence of clustering in the database due to uncertainty in the appropriate magnitude values and an increase in the number of unwanted seismic events.

4.2 Modelling of Seismic Sources

The seismic-tectonic and regionalization maps given in the 2nd progress report were characterized and modelled to 68 point, line, and or area seismic sources for probabilistic computer modelling.

4.2.1 Grids of Seismic Hazard Assessment

The seismic hazard assessment for the Kingdom has been performed for two grid models. The first grid model is referred to thereafter as (Country Model) and the second model is referred to thereafter as (Regional Model). In the Country Model the seismic hazard parameters were calculated at nods of grids intersect at longitude-latitude intervals of 1-degree by 1-degree covering the whole area of Kingdom. The results of this grid model will be utilized to produce the country map of the maximum considered earthquake ground motion in terms of long and short period's spectral response acceleration in counters manner. The Regional Model is based on condense meshing of 0.25 degree by 0.25 degree longitude-latitude intervals of a specific region (i.e. 5 longitudinal degrees X 5 latitudinal degrees for the north-west region of the Kingdom). In order to provide readable and clear maps, country map was divided to 7 parts.

Seismic hazard analysis has been performed for each part considering the most recent seismicity of the Kingdom of Saudi Arabia and neighbouring countries.

4.2.2 Attenuation Relationship

Another of equal important step the study methodology pertained to selection of an appropriate ground motion Attenuation Relationship (AR) for use of the probabilistic seismic hazard assessment at each of the study sites. Several AR,s have been examined and compared with ground motion acceleration data recorded during 1995 Gulf of Aqaba Earthquake. The most relevant AR was found the refined version of the relationships of Sadigh et al (1989) and Sadigh and Chang (1990). The AR table developed for the analysis includes relationships for peak ground acceleration (PGA) and spectral acceleration (SA) for 14 periods of vibration in range of 0.05 to 6 seconds, for moment magnitude (M) in range of 4.4 to 8, and site distance in range of 5 to 500 Km form the seismic sources.

4.3 Results

To this end, all input parameters for earthquake hazard analysis at all study sites were been furnished. The AR table along with the geometry and seismic characteristics of the designated seismic courses were incorporated in computer modeling for probabilistic seismic hazards analysis. The earthquake recurrence parameters of the respected sources were assigned for the different sources based on an inherent uncertainties logic tree distribution. As per the recommendations of section 4.1.3 of NEHRP (2000), the spectral response of ground motion accelerations with 2% probability of being exceeded in 50 years were calculated for both the Country Model and the Regional Model. The results of the Country Model were used for contouring the response spectral accelerations at short period (0.2 second) (S_S), and at 1-second on the whole geographical map of the Kingdom as shown in figure 1(a) & (b), pages 62 & 63 respectively. In order to provide readable and clear maps, the Kingdom's geographic map was divided to 7 parts (regions) as shown in figure 2, page 64. The Regional Model results were used to produce maps of (S_S) and (S_1) with lower contouring levels for each part, as shown in figures 3a, 3b, 4a, 4b, 5a, 5b, 6a, 6b, 7a, 7b, 8a, 8b, 9a & 9b in page 65-78

The following is list containing the maximum considered earthquake for shore & long spectral response acceleration for stations present at, Meteorological and Seismic Design Data SAES-A-112.

	Coordinates		SAES-A-112	
Stations	Long. E	Lat. N	S_S in %g	S_1 in %g
Abha	42 30'	18 12'	20.0	5.4
Abqaiq	49 40'	25 56'	14.6	3.8
Abu Sa'fah	50 30'	26 54'	8.3	2.8
Al-baha	41 27'	20 00'	16.0	4.2
Al-Jauf	40 12'	29 56'	14.5	4.0
Ar'ar	40 59'	30 58'	3.2	0.8
Berri	49 35'	26 57'	15.0	4.0
Dammam	50 06'	26 26'	8.3	2.8
Dhahran	50 06'	26 18'	8.3	2.8
Duba	35 41'	27 21'	26.6	8.5
E/W PS No 3	47 30'	25 10'	0.8	0.2
E/W PS No 6	44 58'	24 42'	14.0	3.6
E/W PS No 10	41 24'	24 05'	5.0	1.0
Hail	41 41'	27 31'	1.2	0.4
Haradh	49 13'	24 03'	16.5	4.2
Hawiyah	49 21'	14 48'	15.0	3.5
Hawtah	46 50'	22 58'	0.6	0.2
Hofuf	49 34'	25 30'	15.9	4.1
Jeddah	39 11'	21 29'	30.6	11.0
Jizan	42 32'	16 54'	43.3	11.3
Ju'aymah	49 56'	26 47'	8.5	2.8
Jubail	49 34'	27 01'	8.3	2.8
Khamis Mashayt	42 43'	18 18'	18.4	4.8
Khurais	48 08'	25 05'	5.0	2.0
Medina Almunawara	39 35'	24 31'	26.9	7.0
Marjan	49 42'	28 27'	8.0	5.0
Najran	44 13'	17 33'	35.2	9.1
Qaisumah	46 07'	28 20'	1.0	0.6
Qasim	43 58'	26 18'	14.0	3.6
Qatif	50 00'	26 30'	8.5	2.8
Rabigh	39 02'	22 48'	16.9	6.2
Ras Tanura	50 05'	26 42'	8.5	2.8
Riyadh	46 52'	24 31'	0.8	0.2
Safaniyah	48 45'	27 59'	7.6	5.0
Shaybah	53 56'	22 30'	5.0	1.0
Shedgum	49 24'	25 36'	8.5	2.8
Tabuk	36 33'	28 23'	27.2	11.0
Tanajib	48 46'	27 52'	7.5	5.0
Turaif	38 40'	31 41'	18.7	4.8
Udhailiyah	49 17'	25 08'	15.0	4.0
Unayzah	43 58'	26 06'	5.0	1.0
Uthmaniyah	49 18'	25 13'	16.0	4.5
Yanbu	38 03'	42 04'	18.3	4.8

Excel Worksheet has been developed for calculation of Design Response Spectrum for specific, values of S_S and S_1, and Soil-Site class. Calculations of the spectral values are based on Section 1615.1.4 of the IBC-03 Code.

The figures 3.a through 9.b page 65-78 show maximum considered earthquake Ground motion spectral response accelerations (S_S and S_1 in %g) mapped for Regions 1to 7 respectively. The part (a) of each figure depicts values of S_S while the part (b) depicts S_1 values of the respected region. It can be seen that cites names are posted on all maps.

Table 4.1 shows printout of the Excel Workbook that is developed for calculation of Design Response Spectrum for specific, values of S_S and S_1, and Soil-Site class. The table shows the instruction for the Worksheet user and of the input. It shows also example of Design Response Spectrum calculated for given, values of S_S and S_1 in %g, and site class as shown in the Worksheet (S_S = 50%g, S_1 = 20%g, and the Site Class is B). The user shall input values of the site coefficients F_a and F_v which are defined respectively in Tables 1615.1.2(1) and (2) of the IBC-03 Code.

Table 4.1 Desgin Response Spectra

Input: The user shall put the following parameters:

S_S in the cell **B12**

S_1 in the cell **D12**

Soil Site Class in the Cell **F12**

Site coefficient F_a in the cell **H12**

Site coefficient F_v in the cell **J12**

Calculations of the spectral values are based on Section 1615.1.4 of the IBC 2003 Code

S_S =	50	S_1 =	20	Soil Site Class=	B	F_a =	1	F_v =	1
S_{DS} =	0.333	S_{MS} =	0.5						
S_{D1} =	0.133	S_{M1} =	0.2						

T,Sec.	Sa
0.000	0.133
0.080	0.333
0.400	0.333
0.450	0.296
0.500	0.267
0.550	0.242
0.600	0.222
0.650	0.205
0.700	0.190
0.750	0.178
0.800	0.167
0.850	0.157
0.900	0.148
0.950	0.140
1.000	0.133
1.050	0.127
1.100	0.121
1.150	0.116
1.200	0.111
1.250	0.107
1.300	0.103
1.350	0.099
1.400	0.095
1.450	0.092
1.500	0.089
1.550	0.086
1.600	0.083
1.650	0.081
1.700	0.078
1.750	0.076
1.800	0.074
1.850	0.072
1.900	0.070
1.950	0.068
2.000	0.067
2.050	0.065
2.100	0.063
2.150	0.062

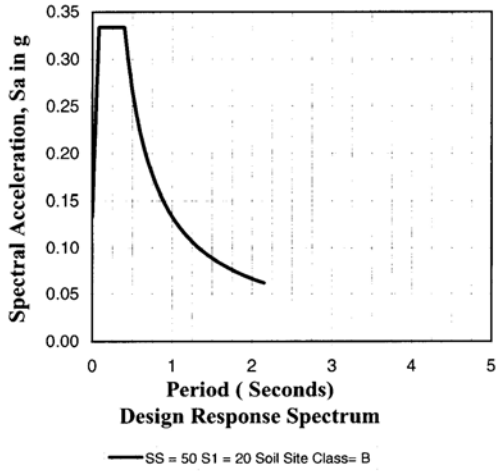

2.200	0.061
2.250	0.059
2.300	0.058
2.350	0.057
2.400	0.056
2.450	0.054
2.500	0.053
2.550	0.052
2.600	0.051
2.650	0.050
2.700	0.049
2.750	0.048
2.800	0.048
2.850	0.047
2.900	0.046

2.950	0.045
3.000	0.044
3.050	0.044
3.100	0.043
3.150	0.042
3.200	0.042
3.250	0.041
3.300	0.040
3.350	0.040
3.400	0.039
3.450	0.039
3.500	0.038
3.550	0.038
3.600	0.037
3.650	0.037

3.700	0.036
3.750	0.036
3.800	0.035
3.850	0.035
3.900	0.034
3.950	0.034
4.000	0.033
4.050	0.033
4.100	0.033
4.150	0.032
4.200	0.032
4.250	0.031
4.300	0.031
4.350	0.031
4.400	0.030

4.450	0.030
4.500	0.030
4.550	0.029
4.600	0.029
4.650	0.029
4.700	0.028
4.750	0.028
4.800	0.028
4.850	0.027
4.900	0.027
4.950	0.027
5.000	0.027
5.050	0.026
5.100	0.026
5.150	0.026
5.200	0.026

CHAPTER 5

CONCLUSIONS AND RECOMMENDATIONS

It can be said that the results of this study raised crucial advancements in the seismic design criteria of the KSA. One aspect of the advancements is the up-to-date probabilistic seismic hazard assessment based on critical interrelated multidisciplinary geological, seismological, and seismotectonic studies of seismic sources that may be of significant effects on evaluation of seismic hazard in the Kingdom. This showed up significant changes in seismic hazard predicted by similar previous studies in some areas of the Kingdome.

The other significant outcome of the study is preparation of design ground motion parameters (maximum considered earthquake spectral response acceleration at short period "S_s" & long period "S_1") consistent with IBC-03, which is considered as the basic-code for the Saudi Building Code (SBC). Maps of this study are therefore essential for the SBC to adopt the IBC seismic provisions for building design in the Kingdom. The IBC adopts an approach provides balance between the risk level and the costs, as the selection of the seismic design category is based on three parameters: the spectral acceleration values, the occupancy category of the building, and soil-site class (in term of S_D), see tables 1616.3 (1) and (2) of UBC-03. This is more reliable approach than that of UBC, which base the design category only on the zone factor (Z). This implies that the outcome of this study will have positive impact on seismic design considerations in the Kingdome. On this context, Table 5.1 demonstrates this point. It can be seen that the UBC provides only on design category (IMRF) for all types of buildings regardless the soil-site class, while IBC provides three types of design categories, see tables 1616.3 (1) and (2) of UBC-03. This implies that the outcome of this study will have positive impact on seismic design considerations in the Kingdome.

Table 5.1 Design Categories for Jizan City

Site-Soil Class	Code	Occupancy Category		
		Standard	Special	Essential
B	UBC	IMRF	IMRF	IMRF
	IBC	ORMF^{+}	ORMF+	IMRF
E	UBC	IMRF	IMRF	IMRF
	IBC	IMRF	IMRF	SMRF

Although the results indicate that the seismic hazard in the eastern province is considerably low, certain parts of this province, contrary to the previous thought, are subjected to seismic design consideration in accordance with IBC code. Specifically, designs of buildings and essential facilities located inside the S_s contour line of 10 shall satisfy the following seismic design categories:

a) Design Category A for all types of buildings and structures located on soil type D or higher quality soil (A, and B)
b) Design Category B for buildings of Standard and Special occupancy categories and located on soil type E.
c) Design Category C for buildings or structures of essential occupancy categories and located on soil type E.

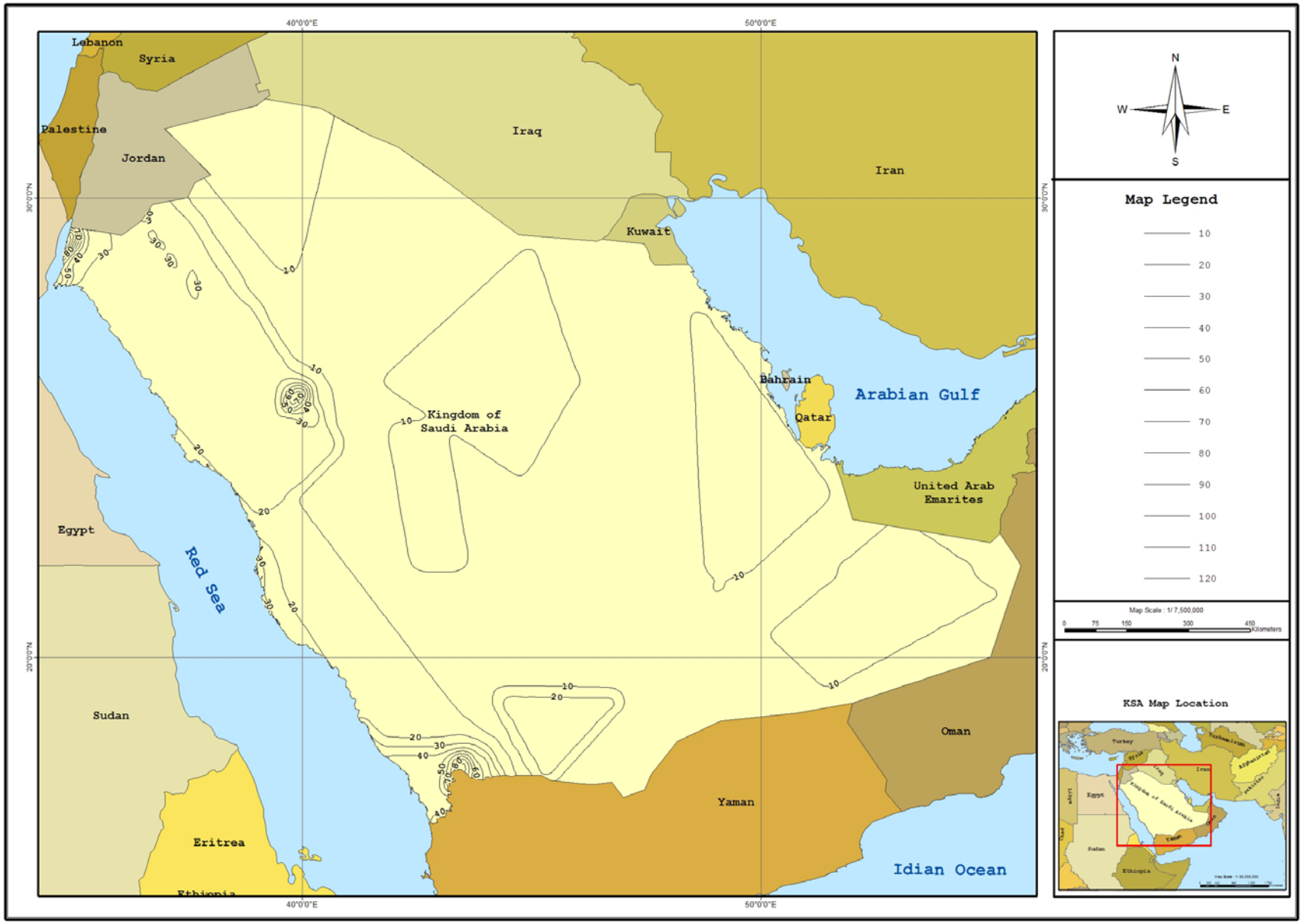

Figure 1(a)

Maximum Considered Earthquake Ground Motion for the Kingdom of 0.2 SEC Spectral Response Acceleration in %g (5 Percent of Critical Damping, Site Class B

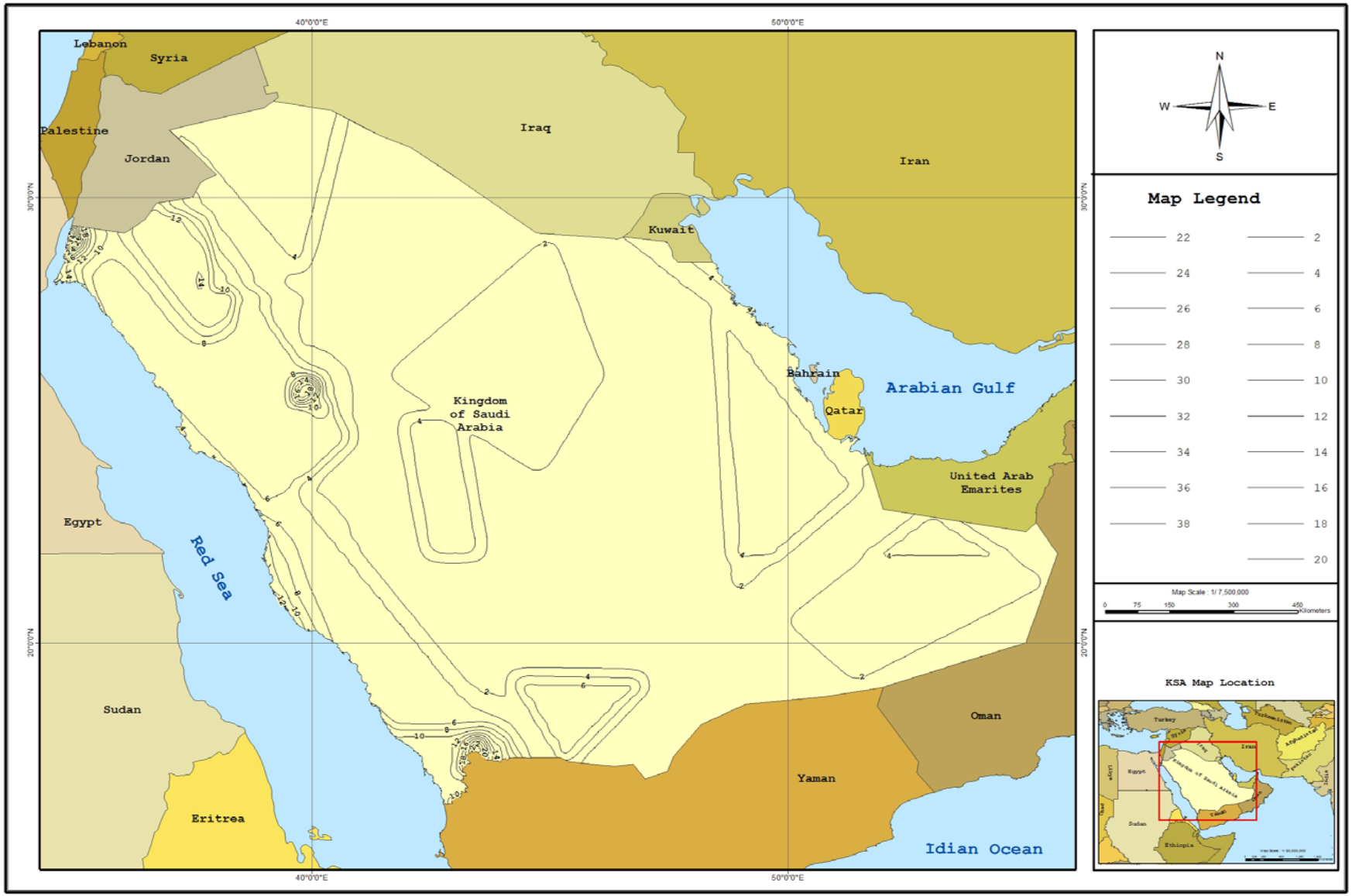

Figure 1(b)

Maximum Considered Earthquake Ground Motion for the Kingdom of 1.0 SEC Spectral Response Acceleration in %g (5 Percent of Critical Damping, Site Class B

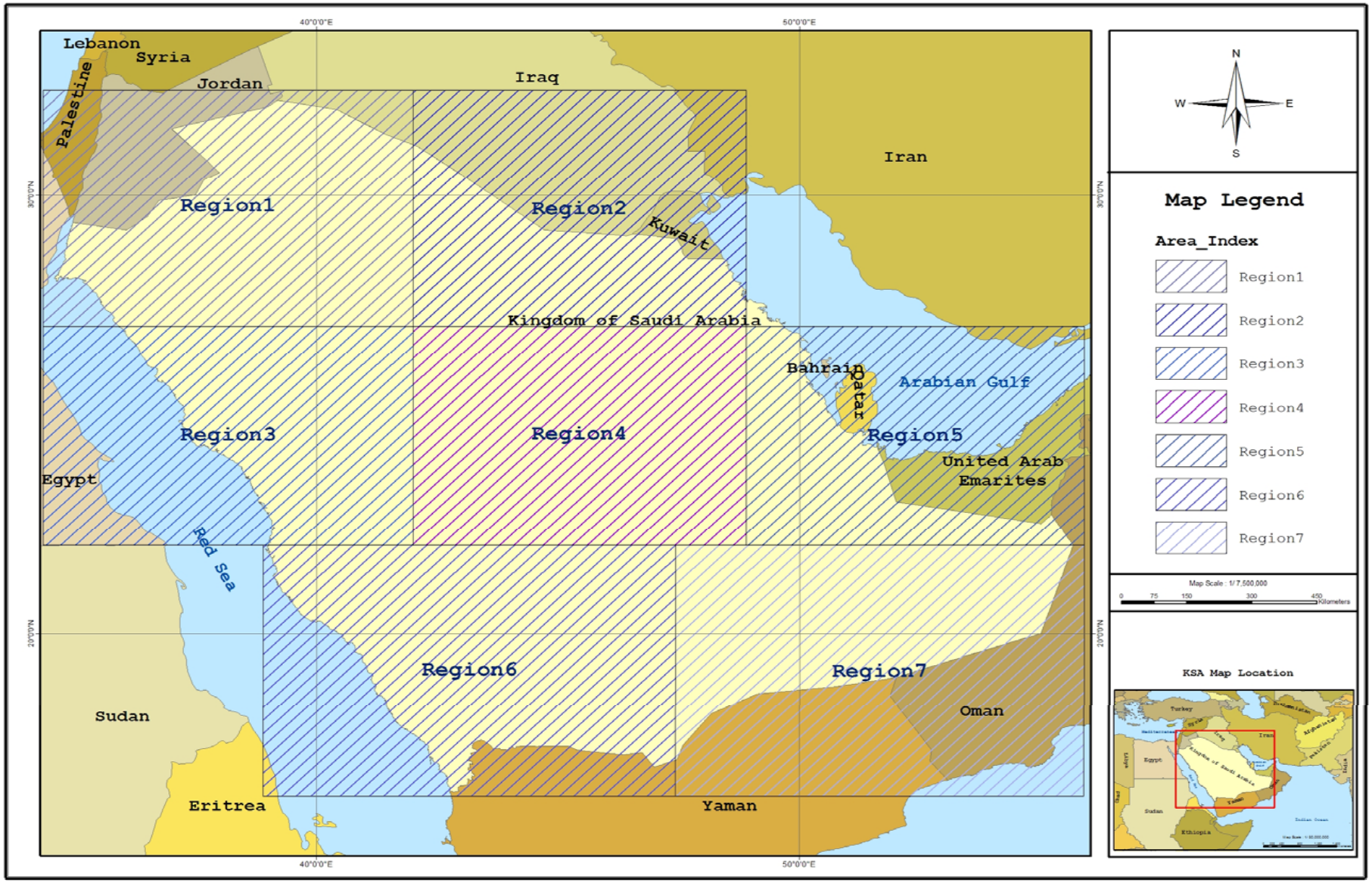

Figure 2
Designations of the Regional maps

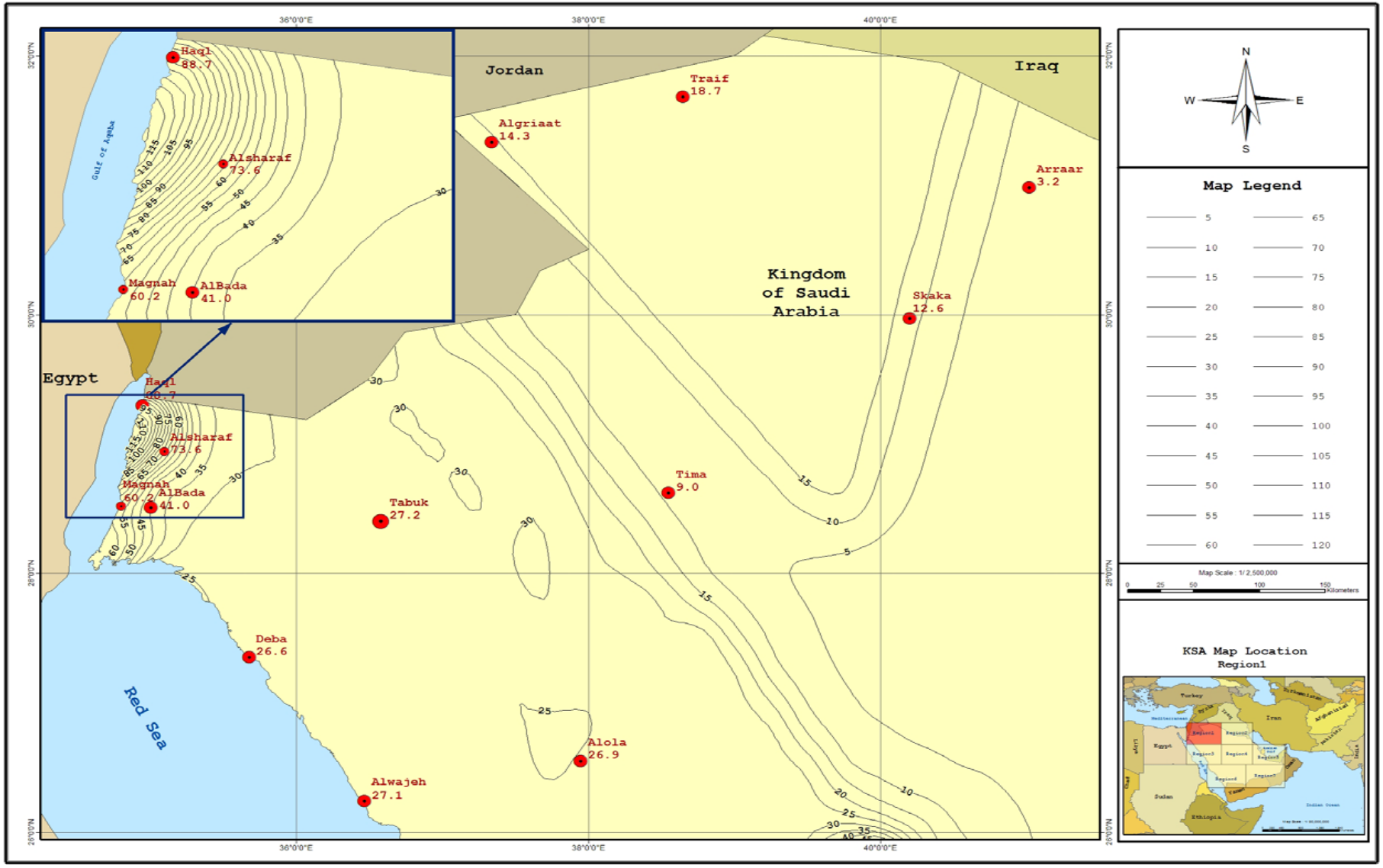

Figure 3(a)

Maximum Considered Earthquake Ground Motion for Region 1 of 0.2 SEC Spectral Response Acceleration in %g (5 Percent of Critical Damping, Site Class B

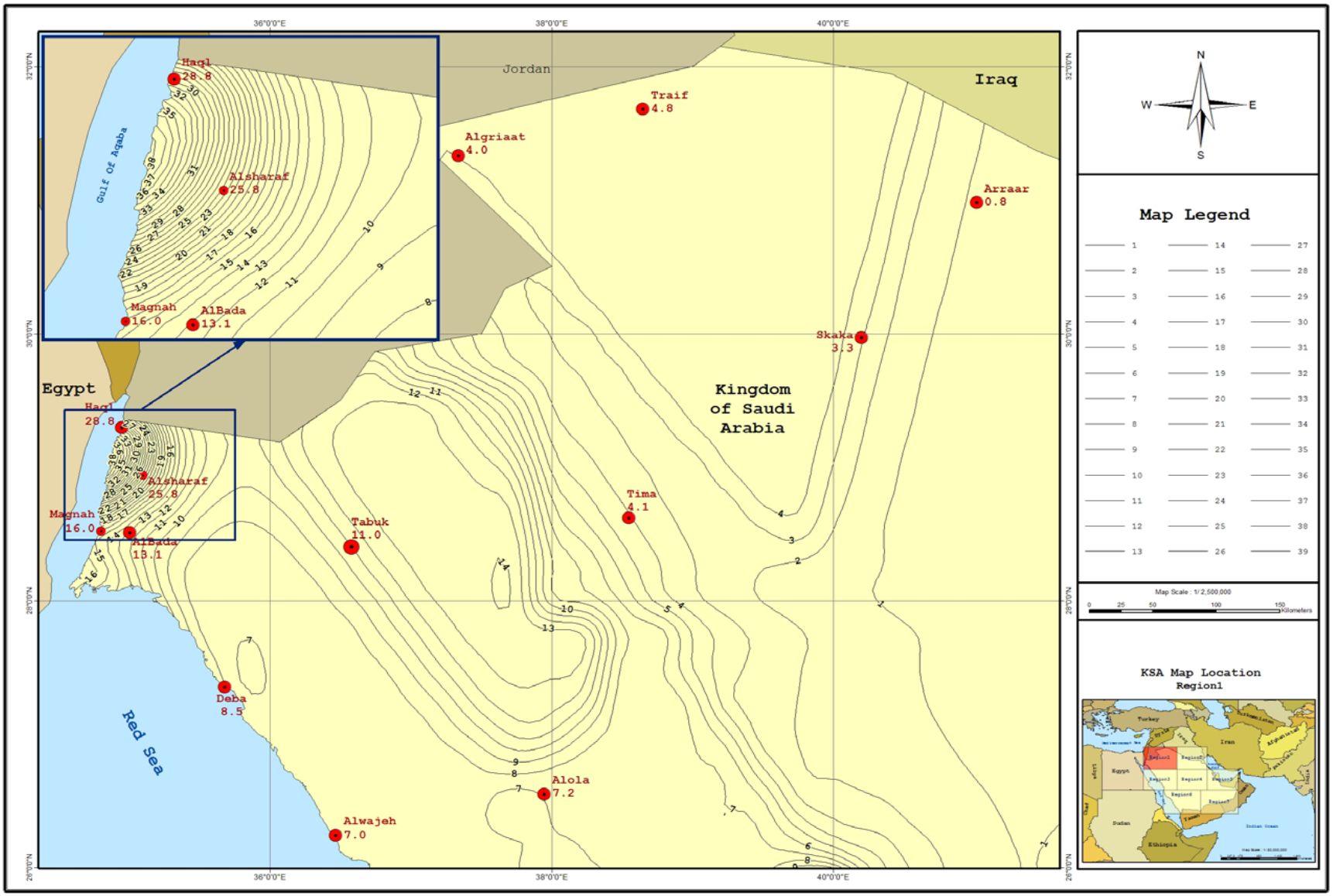

Figure 3(b)

Maximum Considered Earthquake Ground Motion for Region 1 of 1.0 SEC Spectral Response Acceleration in %g (5 Percent of Critical Damping, Site Class B)

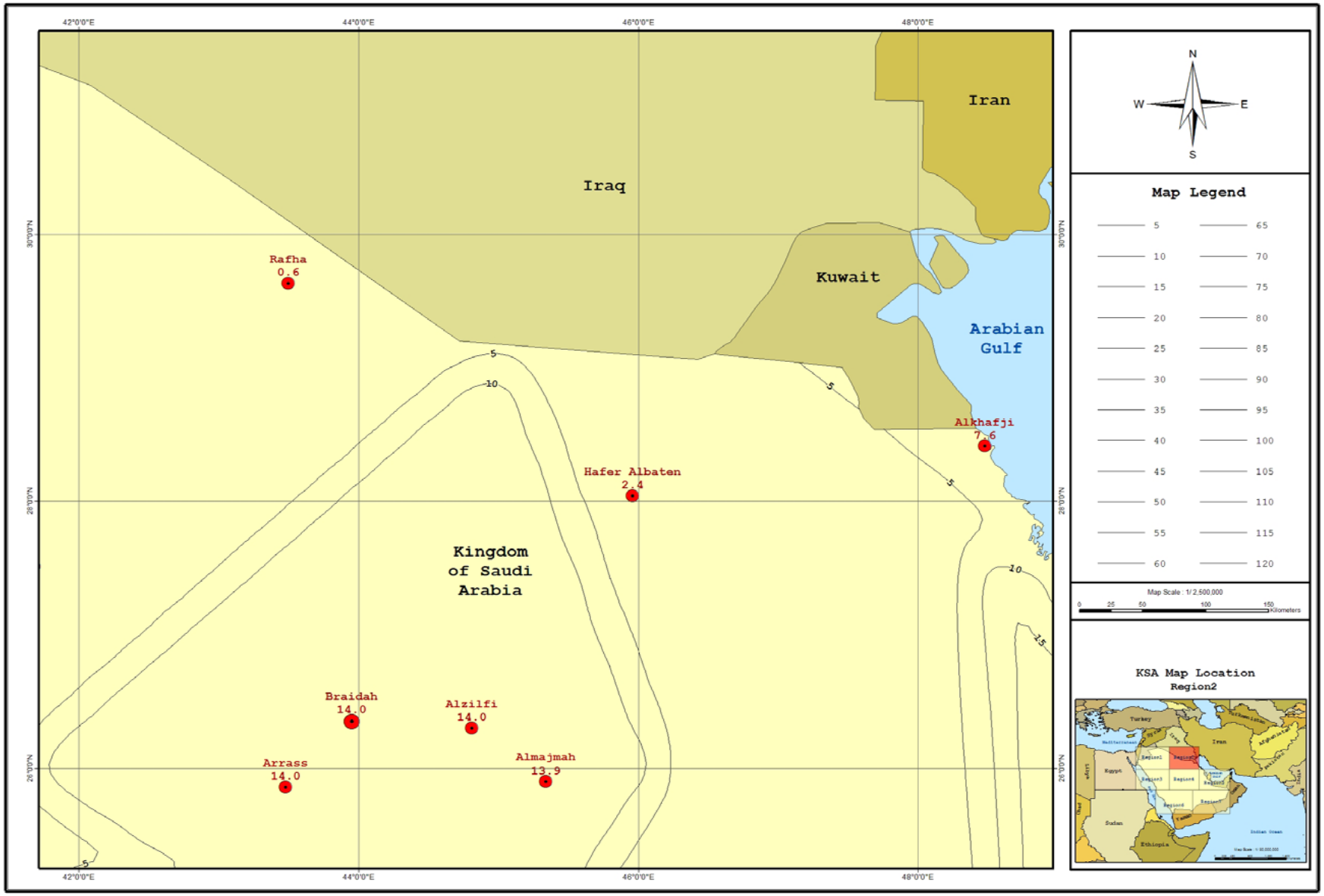

Figure 4(a)

Maximum Considered Earthquake Ground Motion for Region 2 of 0.2 SEC Spectral Response Acceleration in %g (5 Percent of Critical Damping, Site Class B

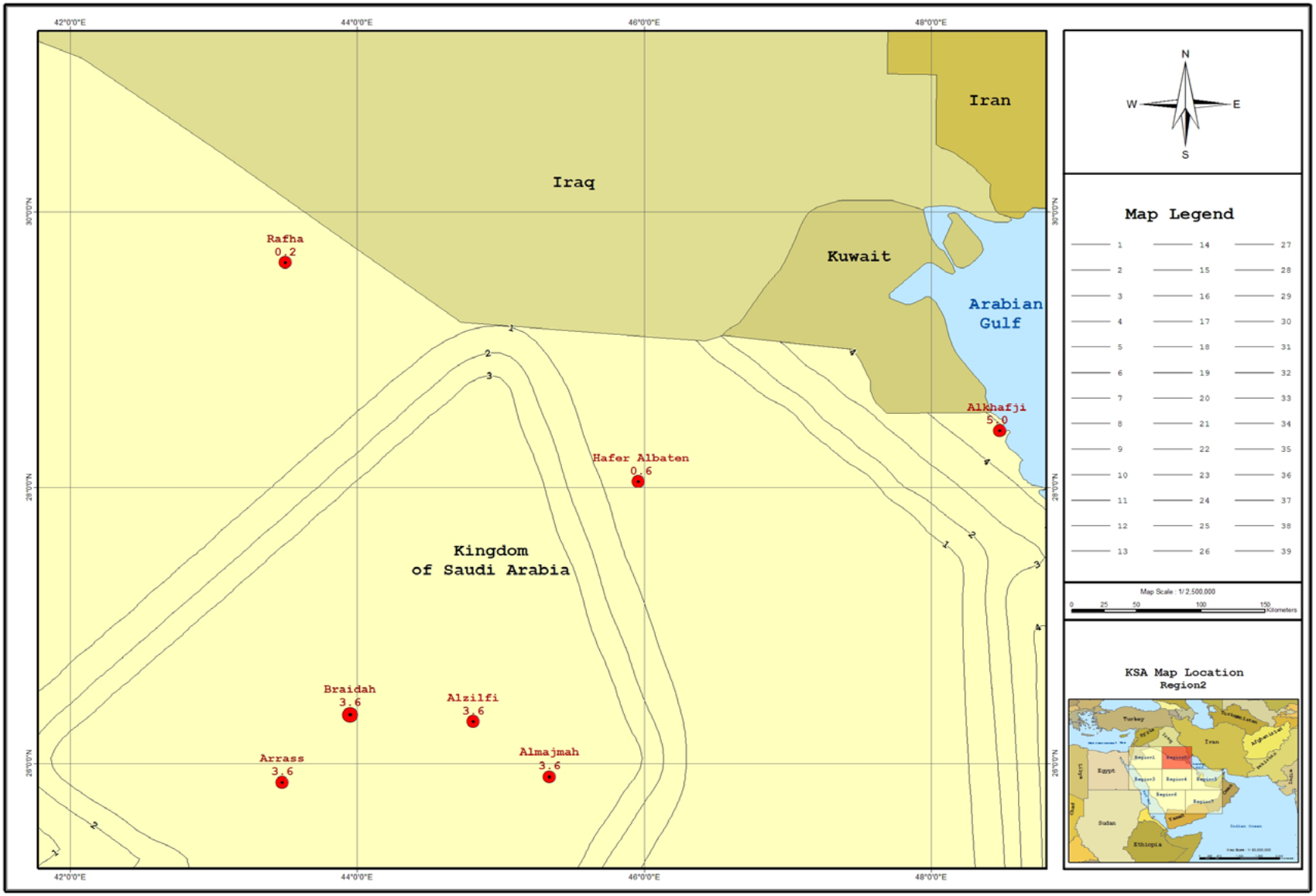

Figure 4(b)

Maximum Considered Earthquake Ground Motion for Region 2 of 1.0 SEC Spectral Response Acceleration in %g (5 Percent of Critical Damping, Site Class B)

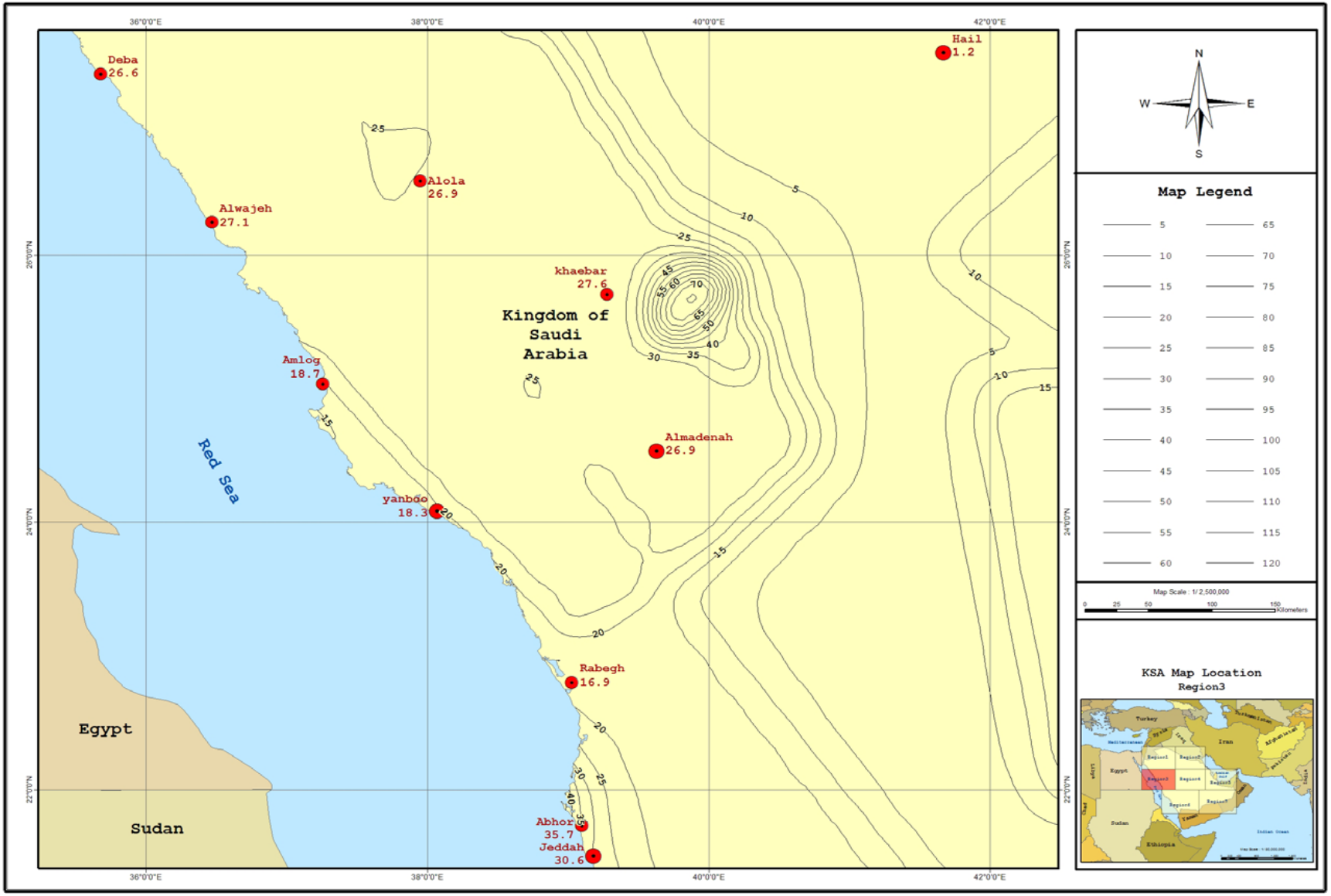

Figure 5(a)

Maximum Considered Earthquake Ground Motion for Region 3of 0.2 SEC Spectral Response Acceleration in %g (5 Percent of Critical Damping, Site Class B)

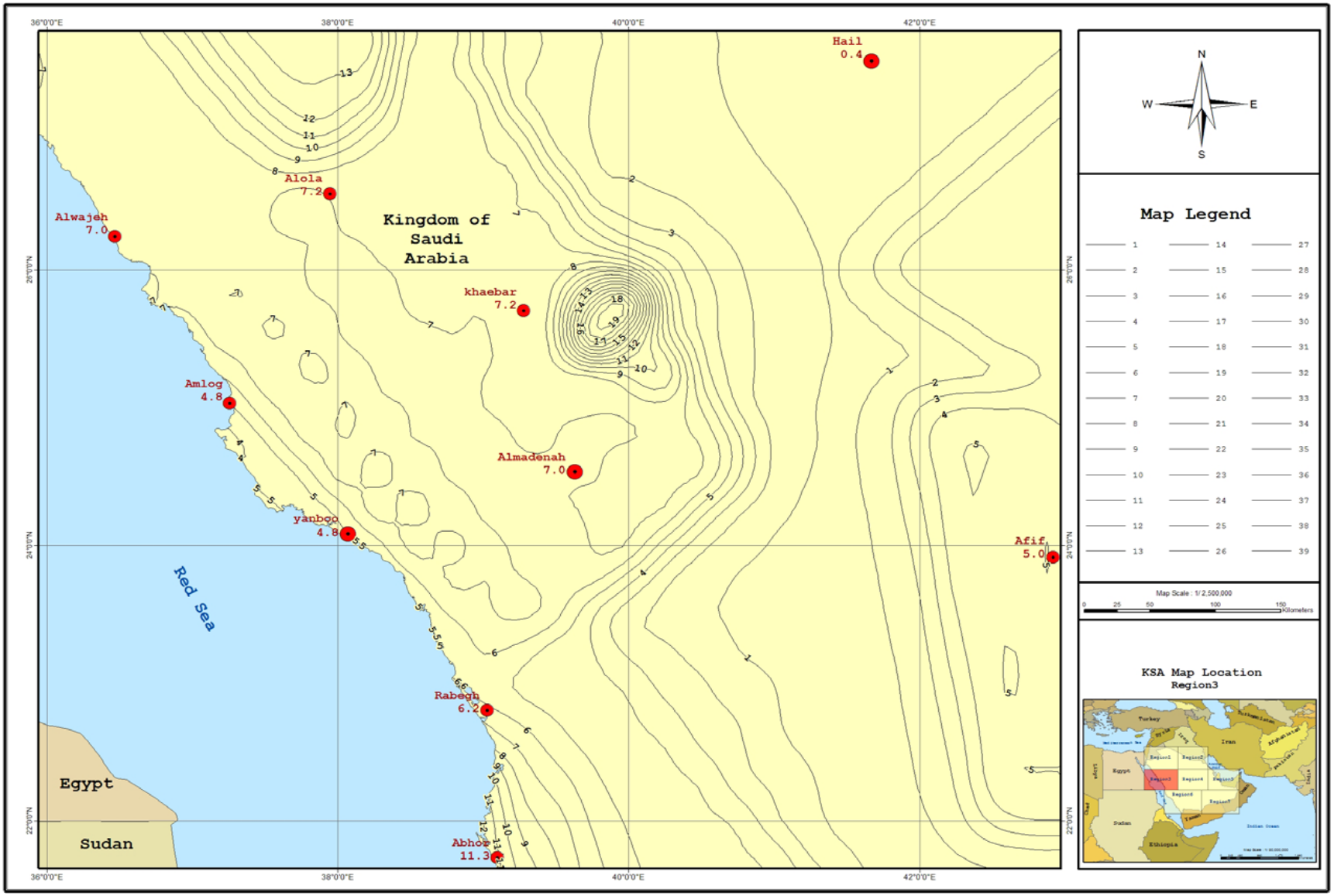

Figure 5(b)

Maximum Considered Earthquake Ground Motion for Region 3of 1.0 Sec Spectral Response Acceleration in %g (5 Percent of Critical Damping, Site Class B)

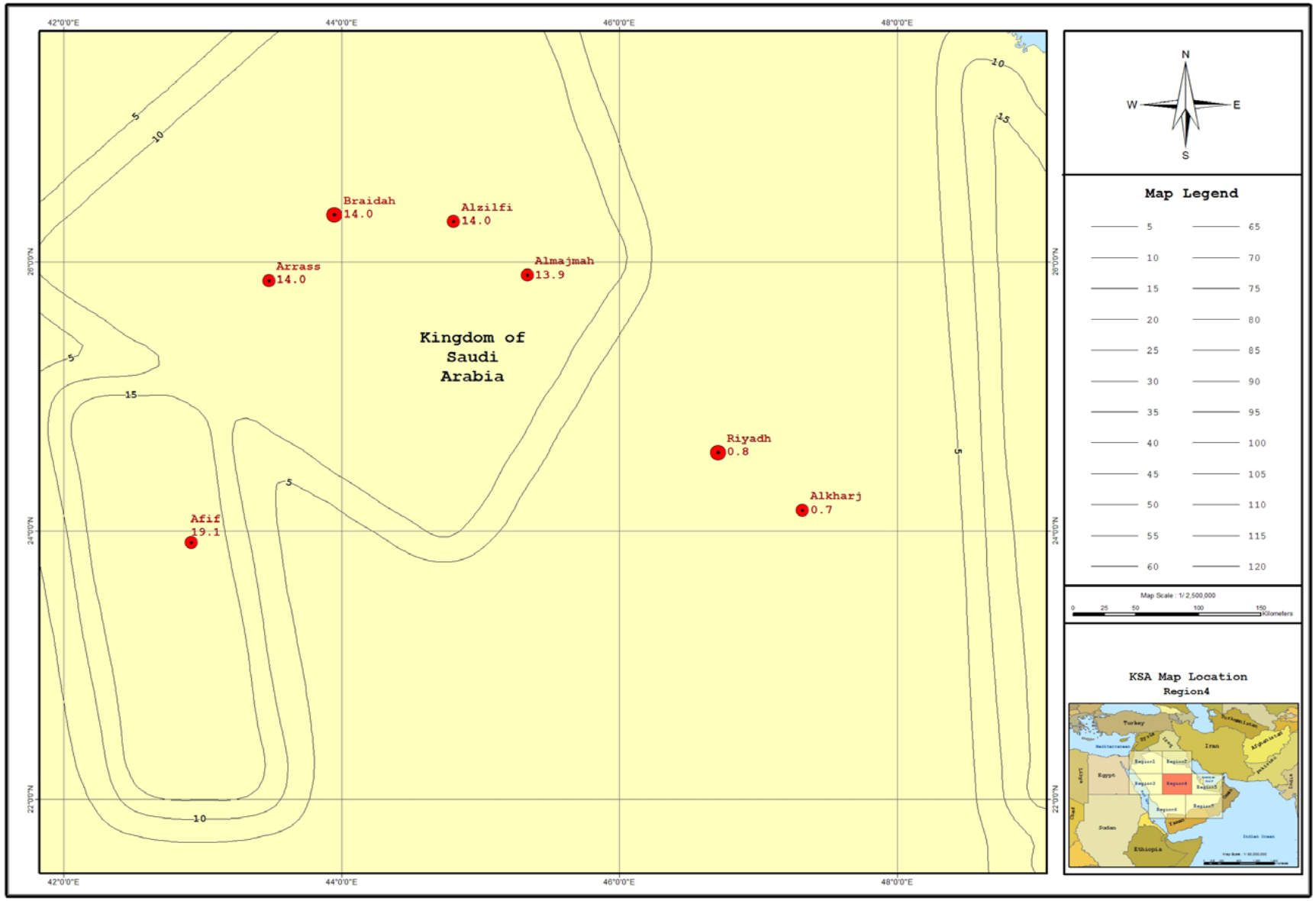

Figure 6(a)

Maximum Considered Earthquake Ground Motion for Region 4of 0.2 SEC Spectral Response Acceleration in %g (5 Percent of Critical Damping, Site Class B)

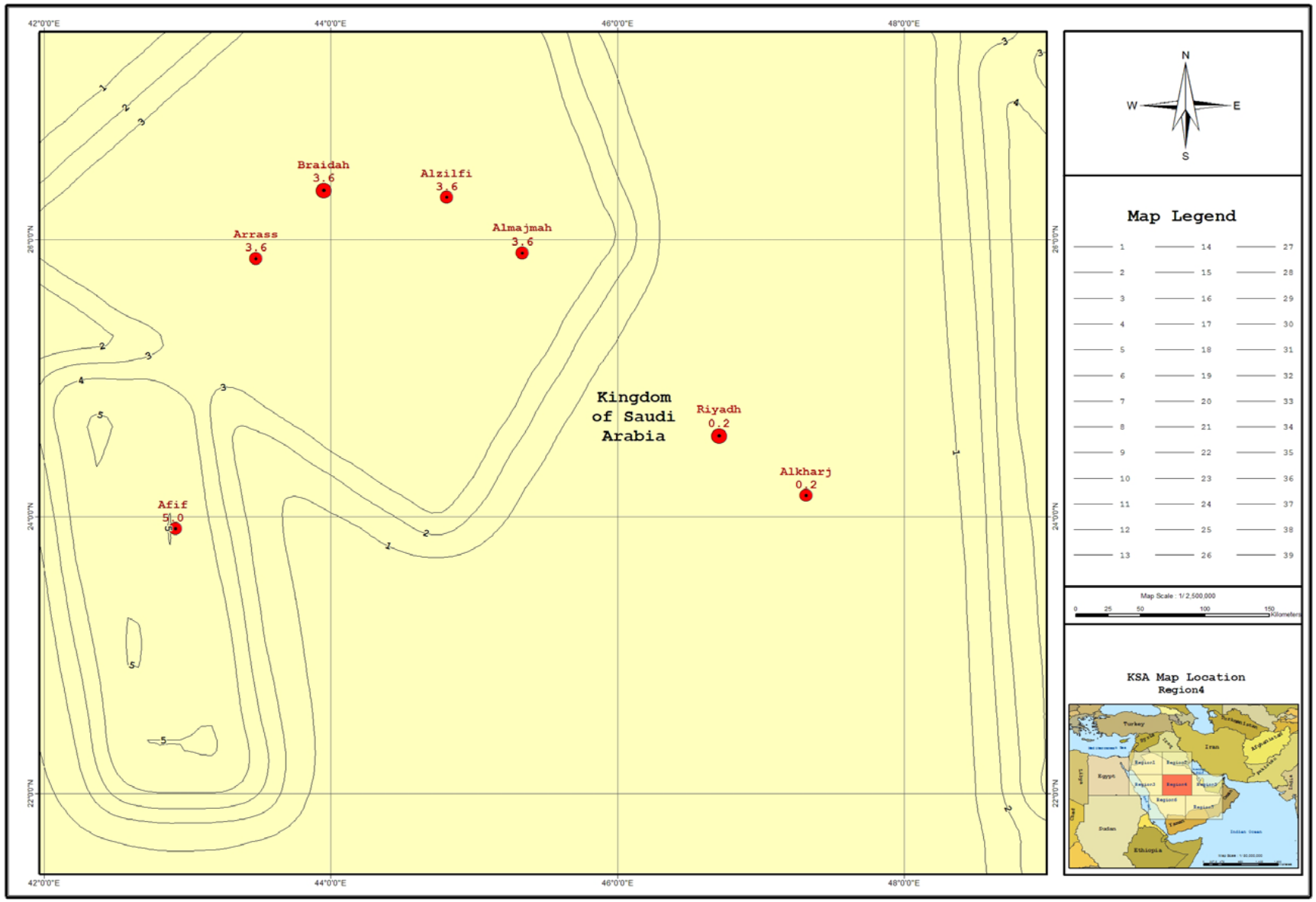

Figure 6(b)
Maximum Considered Earthquake Ground Motion for Region 4of 1.0 SEC Spectral Response Acceleration in %g (5 Percent of Critical Damping, Site Class B)

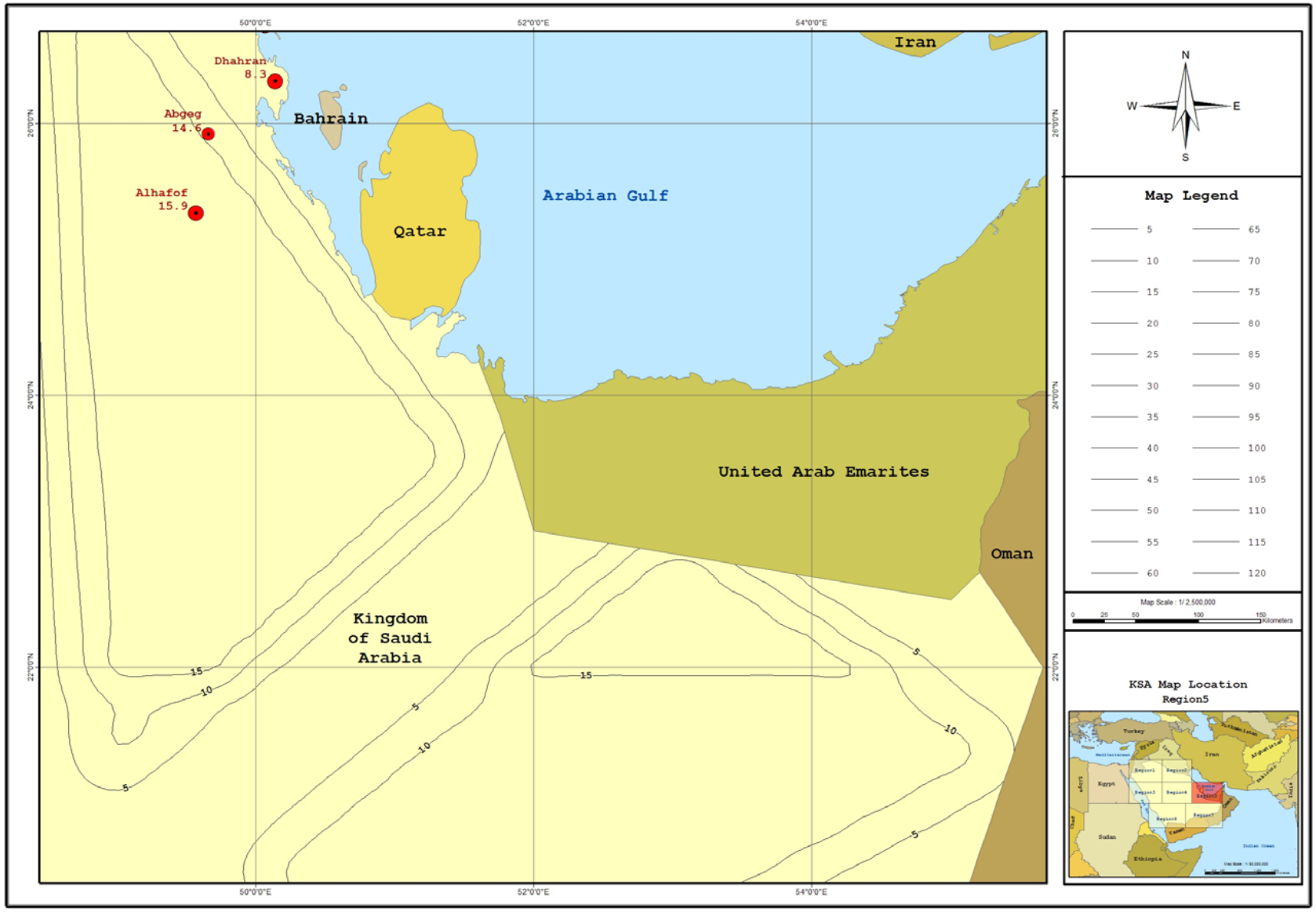

Figure 7(a)
Maximum Considered Earthquake Ground Motion for Region 5of 0.2 SEC Spectral Response Acceleration in %g (5 Percent of Critical Damping, Site Class B)

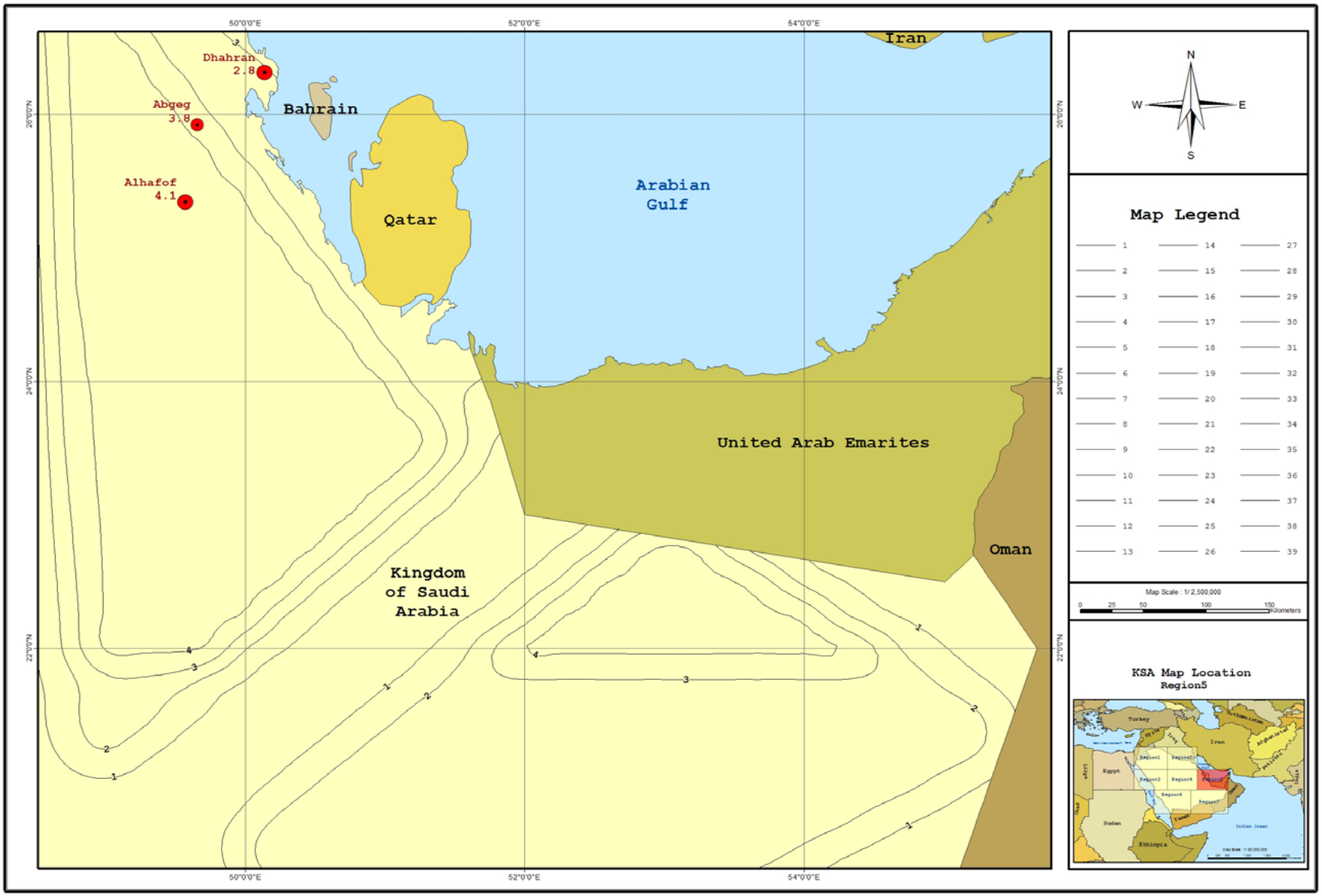

Figure 7(b)

Maximum Considered Earthquake Ground Motion for Region 5of 1.0 SEC Spectral Response Acceleration in %g (5 Percent of Critical Damping, Site Class B)

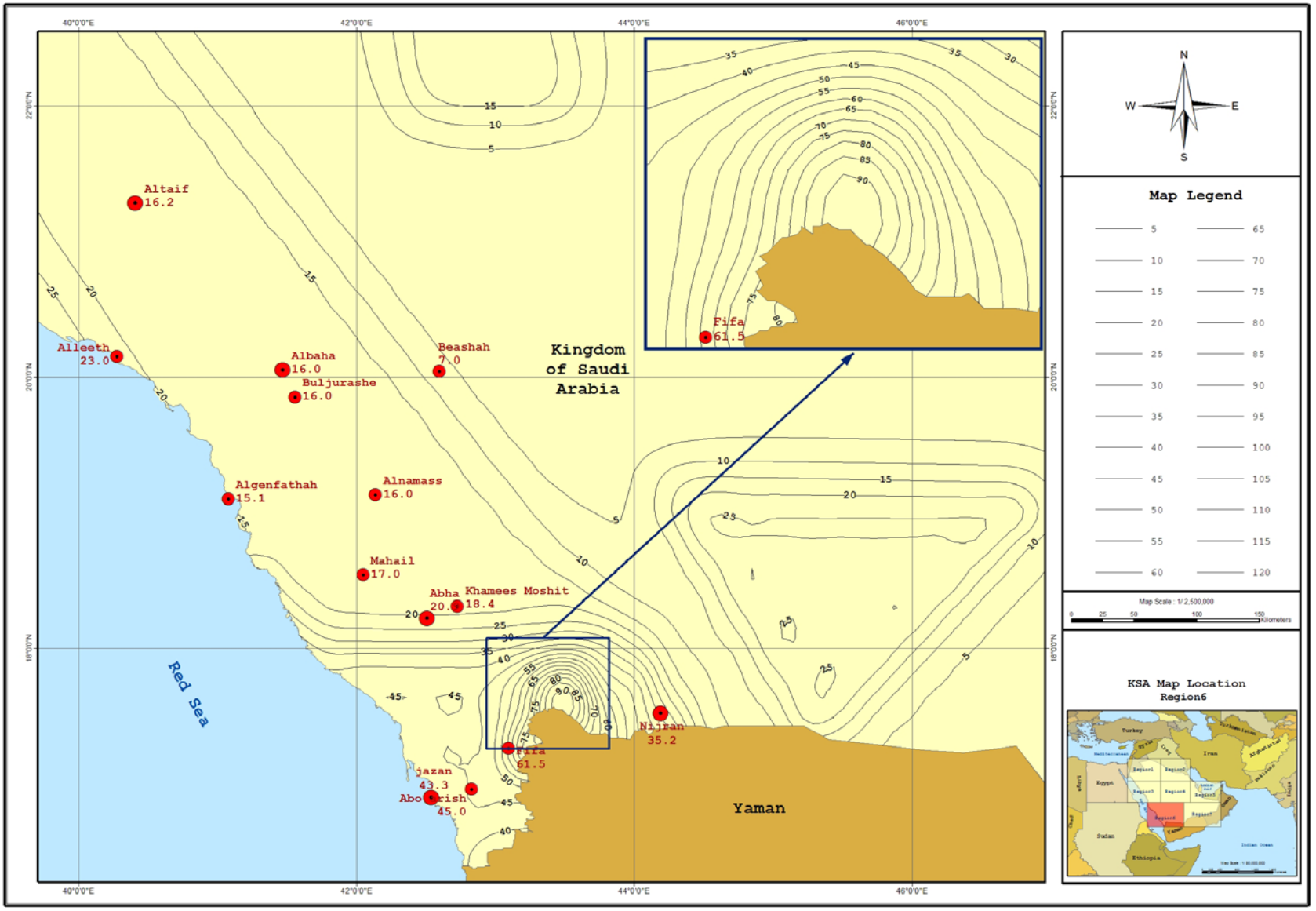

Figure 8(a)
Maximum Considered Earthquake Ground Motion for Region 6of 0.2 SEC Spectral Response Acceleration in %g (5 Percent of Critical Damping, Site Class B)

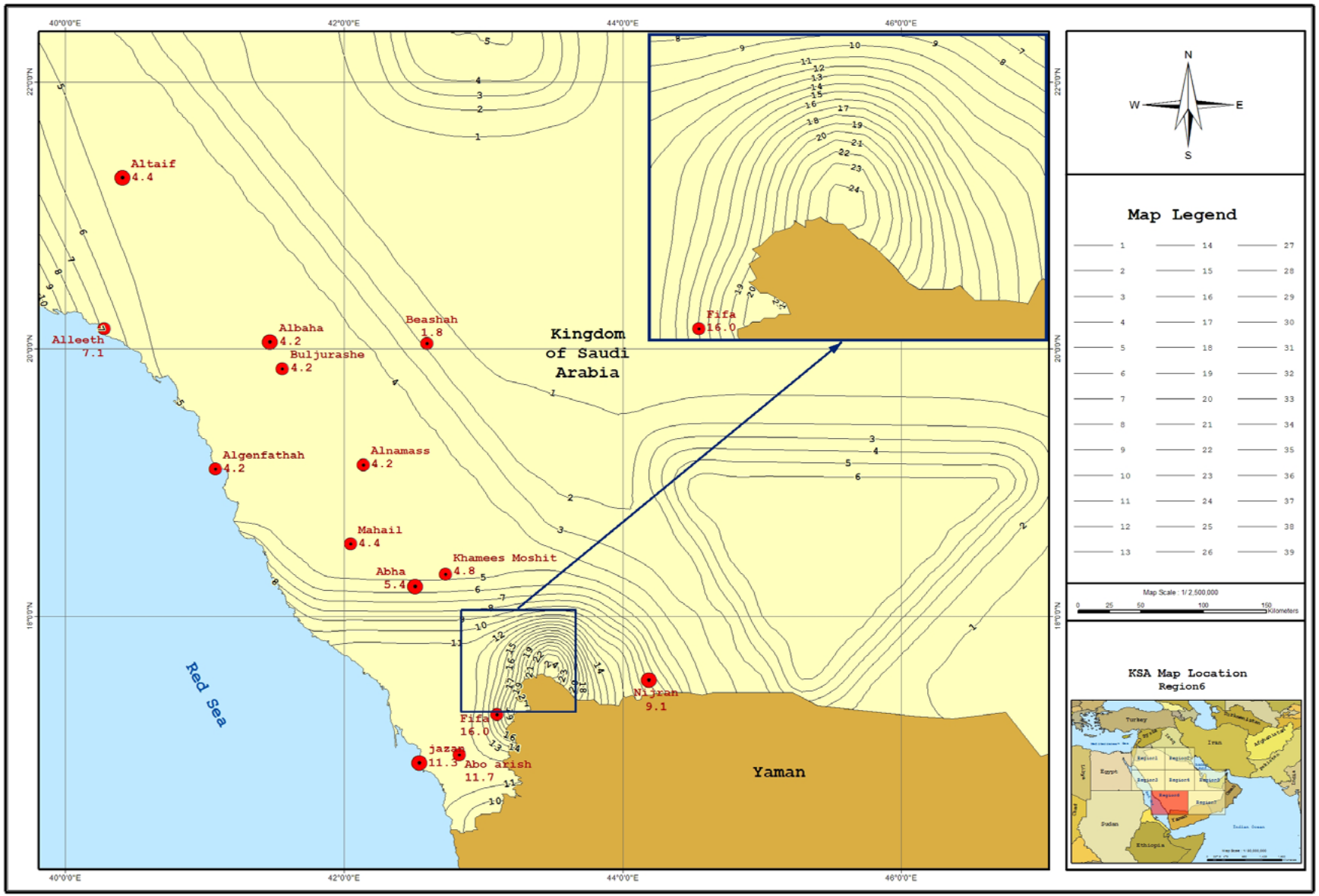

Figure 8(b)
Maximum Considered Earthquake Ground Motion for Region 6of 1.0 SEC Spectral Response Acceleration in %g (5 Percent of Critical Damping, Site Class B)

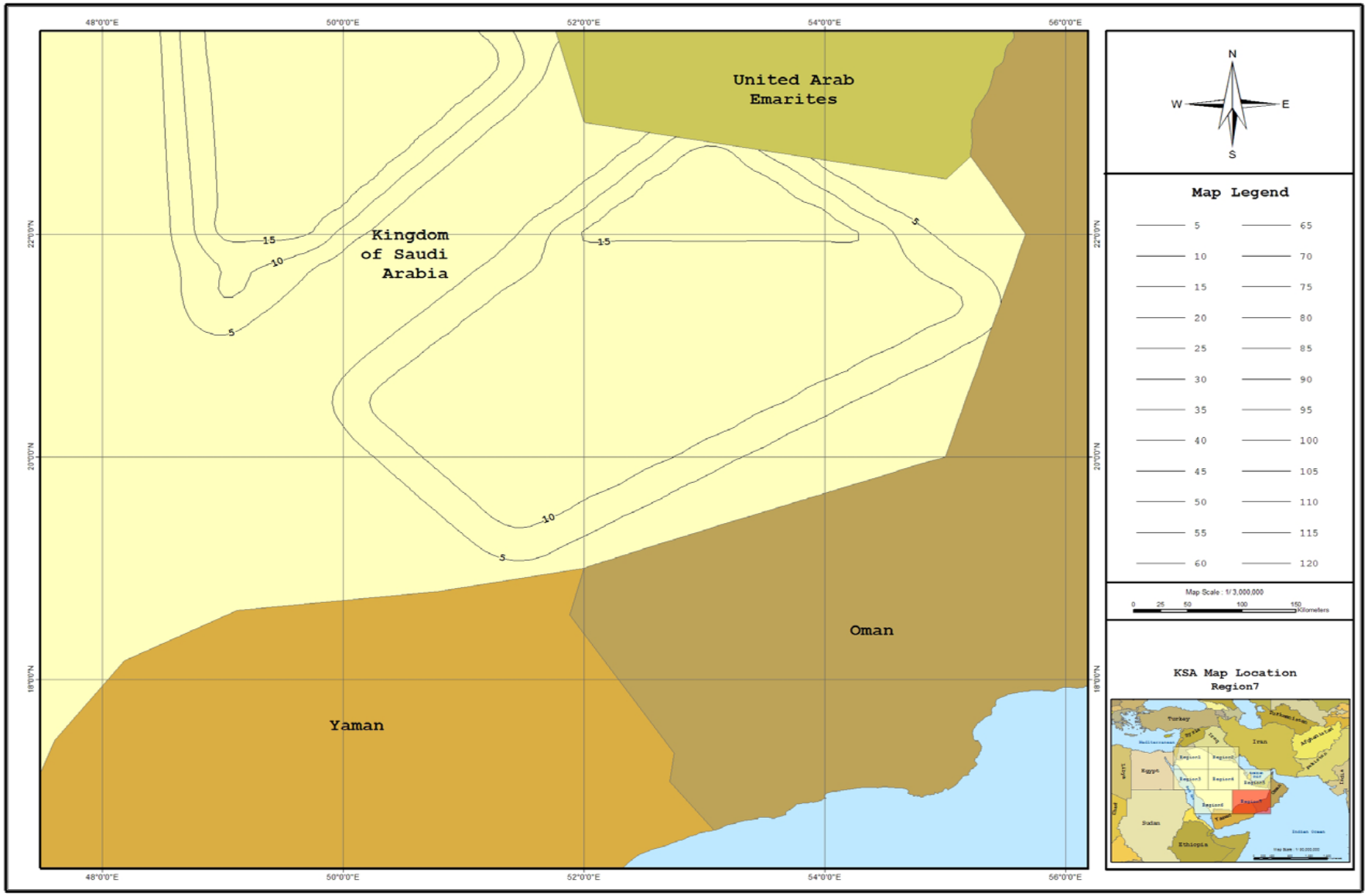

Figure 9(a)

Maximum Considered Earthquake Ground Motion for Region 7of 0.2 SEC Spectral Response Acceleration in %g (5 Percent of Critical Damping, Site Class B)

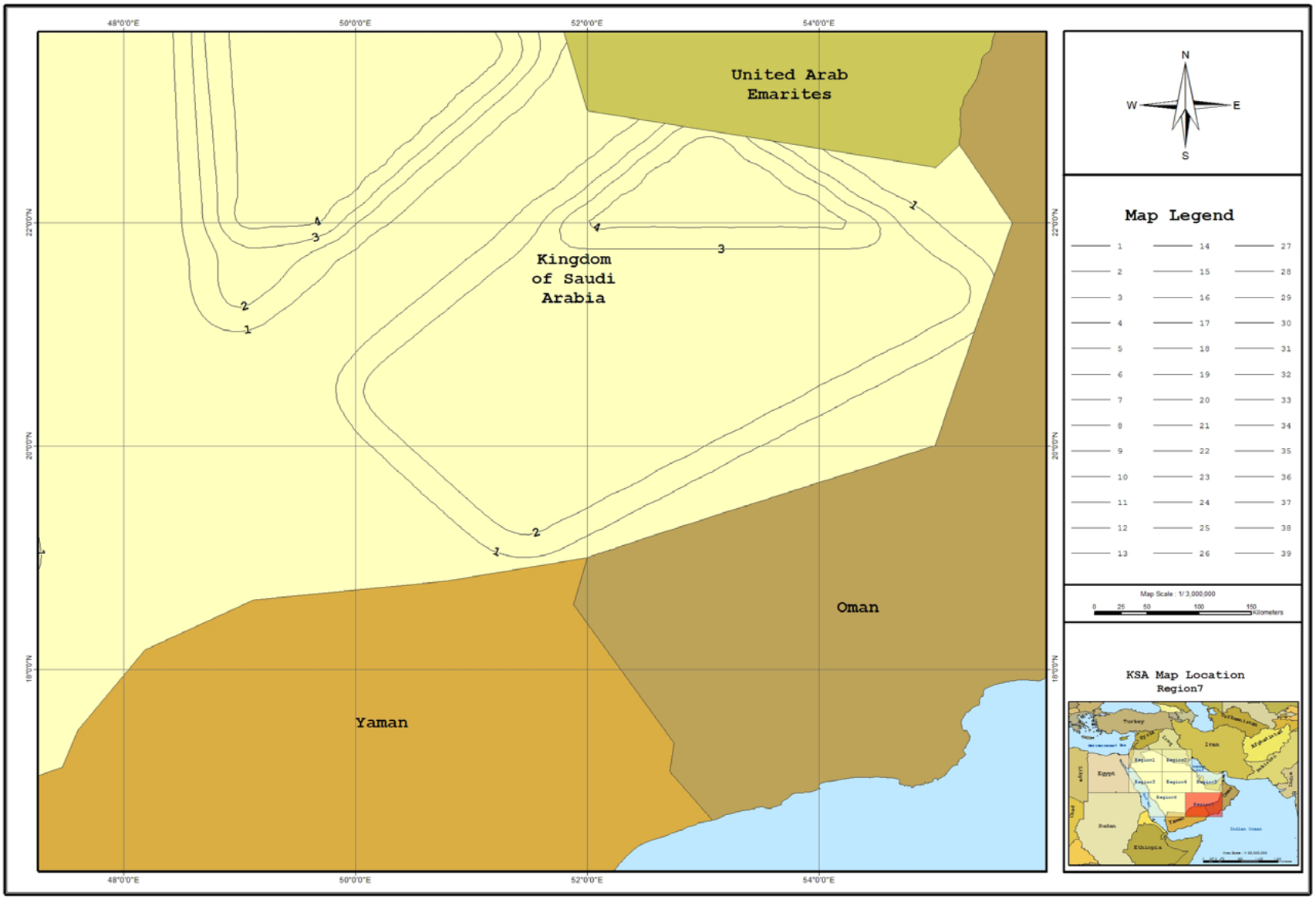

Figure 9(b)
Maximum Considered Earthquake Ground Motion for Region 7of 1.0 SEC Spectral Response Acceleration in %g (5 Percent of Critical Damping, Site Class B)

REFERENCES

Aki K (1965) Maximumlikelihood estimate of b value in the formula logN=a-bM and its confidence limits, Bull. Earthq. Res. Inst., 43, 237-240

Aki K and Richards P (1980) Quantitative Seismology, Theory and Methods, Freeman & Comp., San Francisco, USA

Al-Amri A (1994) Seismicity of the southwestern region of the Arabian shield and southern Red Sea, Jour. Afr. Earth Sc., 19, 17-25

Al-Amri M, Punsalan B and Uy E (1998) Spatial distribution of the seismicity parameters in the Red Sea regions, J. Asian Sc., 16, 557-563.

Al-Fares,A., Bouman, M. and Jeans, P. (1998). A new look at the middle to lower Cretaceous stratigraphy, offshore Kuwait. GeoArabia, V.3, no.4, p. 543-560.

Allen C (1975) Geological criteria for evaluating seismicity, Bull. Geol. Soc. Am., 86, 1041-1057

Ambraseys N (1988) The seismicity of Saudi Arabia and adjacent areas, Report 88/11, 294p, Eng Seismo. Earthq. Eng., Imperial Coll. Of Sc. And Techno., London, UK

Andrews I J (1991) Paleozoic lithostratigraphy in the sub-surface of Jordan, Jordanian Ministry of Energy and Mineral Resources,National Resources Authority, Subsurface Geology,Bull.2, 75p

Barazangi M (1986) Deep structure of the Zagros collision zone: Implication for earthquake hazard assessment and for the spatial distribution of oil fields in the Arabian gulf region, Proc. 3rd Arab Symp. Earthq. Seismo., 35-45

Bender F (1982) On the evaluation of wadi Araba-Jordan rift, Jahrbuch der Geologischen Bundesanstaldt Wien, 4, 3-20

Brown G F and Jackson R O (1960) The Arabian shield, 21st Inter. Geolo. Congr., Copenhagen, 69-77

Brown G F (1972) Tectonic map of the Arabian Peninsula: Saudi Arabian Directorate General of Mineral Resources Arabian Peninsula map AP-2, scale 1: 4,000,000

Brown G F, Schmidt D L, Huffman A C (1989) Geology of the Saudi Arabian peninsula: Shield area of western Saudi Arabia, USGS Professional paper 560-A

Brune J (1969) Seismic moment, seismicity and rate of slip along major fault zones, J. Geophys. Res., 73, 777-784.

Burridge R and Knopoff L (1964) Body force equivalent for seismic dislocation, Bull. Seismo. Soc. Am., 54, 1787-1888.

Dyer R A and Husseini M (1991) The western Rub Al Khali Infracambrian Graben system, Soc. of Petroleum Engr. Paper 21396

Faqira M I and Al-Hauwaj A Y (1998) Infracambrian salt basin in the western Rub Al Khali, Saudi Arabia, GeoArabia (Abstract), 3(1), p93

Gubin I (1967) Earthquake and seismic zoning, Bull. Inter. Inst. Seismo. Earthq. Engg., 4, 107-126

Gutenberg H and Richter C (1954), Seismicity of the Earth, Princeton Univ. Press, New Jersey, USA.

International Building Code 2003 (IBC-03), (2002), International Code Council (ICC), Falls Church, Virginia.

Hank T and Kanamori H (1979) A moment magnitude scale, Jour. Geophys. Res., 84, 2348-2350

Haskell N (1964) Total energy spectra density of elastic waves for propagating faults, Bull. Seismo. Soc. Am., 54, 1811-1841.

Husseini M I (2000) Origin of the Arabian plate structures: Amar collision and Najd rift, GeoArabia, 5(4), 527-542

International Building Code 2003 (IBC-03), (2002), International Code Council (ICC), Falls Church, Virginia.

Johnson P R and Stewart I C F (1994) Magnetically inferred basement structure in central Arabia, Tectonophysics, 245, 37-52

Kanamori H (1977) The energy release in great earthquakes, J. Geophys. Res., 82, 2981-2987.
Keilis-Borok V (1959) On the estimation of the displacement in an earthquake source and source dimensions, Ann. Geofis., 12, 205-214.

Lomnitz C (1974) Global tectonics and earthquake risk, Development in Geotectonic, Elsevier Sci. Publ. Comp., New York, USA

Looseveld R J H, Bell A, Terken J J M (1996) The tectonic evolution of interior Oman, GeoArabia, 1 (1), 28-51

Matsuda T (1975) Magnitude and recurrence interval of earthquakes from a fault, Jour. Seismo. Japan, Ser. 2, 28, 269-283

Mogi K (1962) Study of the elastic shocks caused by the fracture of heterogenous materials and its relation to earthquake phenomena, Bull. Earthq. Res. Inst., 40, 125-173

Moore Mc m J (1979) Tectonics of the Najd transcurrent fault system, Jour. Geol. Soc. London, 136, 441-454

NEHRP (200), Recommended Provisions for the Development of Seismic Regulations for New Buildings, Building Seismic Safety Council, Washington, D.C., 2000

Nolan S C, Skelton P W, Clissold B P, Smewing V D (1990) Maastrichtian to early Tertiary stratigraphy and paleogeography of the central and northern Oman mountains: eds., Robertson A H F, Searle M P, Ries A C, The geology and tectonics of the Oman region, Geol. Soc. London Spec. Publ., 49, 495-519.

Norris D K (1958) Structural conditions in Canadian coal mines: Geological Survey of Canada Bull., 44, 1-53

Noweir M A and Alsharhan A S (2000) Structural style and stratigraphy of the Huwayyah anticline: An example of an Al-Ain Tertiary fold, northern Oman mountains, GeoArabia, 5(3), 387-402

Powers R W, Ramirez L F, Redmond C D, Elberg E L (1966) Geology of the Arabian Peninsula, Sedimentary geology of Saudi Arabia: U. S. Geolog. Survey professional paper 560-D D1-D147

Reid H (1911) The elastic rebound theory of earthquakes, Univ. California, Dept. Geol. Bull., 6 (19), 413-444.

Robertson A H F (1987) Upper Cretaceous muti formation: Transition of a Mesozoic carbonate platform to a foreland basin in the Oman mountains, Sedimentology, 34, 1123-1142

Sadigh K, Chang C Y, Makdisi F, and Egan J A (1989) Attenuation relationships for horizontal peak ground acceleration and response spectra acceleration for rock sites (abs.) , Seismological Research Letters, v. 60, no 1, p. 19.

Sadigh K, Chang C Y (1990) Response spectral relationships for rock, deep-stiff soil, and soft soil site condition, Seismological Research Letters, v. 61, no 1.

Scholz C (1968) The frequency-magnitude relation of micro-fracturing in rock and its relation to earthquakes, Bull. Seismo. Soc. Am., 58, 399-416.

Scholz C (1982) Scaling laws for large earthquakes: Consequences for physical models, Bull. Seism. Soc. Am., 72, 1-14

Slemmons D (1981) A procedure for analyzing the activity of faults, Proc. 3rd Conf. Basement Tectonics, Denver, USA, 33-49.

Stern R and Hedge C E (1985) Geochronological and isotopes constraints on late Precambrian crustal evolution in the eastern desert of Egypt, Am. Jour. Sc., 185, 97-127

Stoeser D B and Camp V E (1985) Pan African Microplate accretion of the Arabian shield, Geol. Soc. Am. Bull., 96, 817-826

Utsu T (1965) A method for determining the value of b in a formula logn=a-bM showing the magnitude-frequency relation for earthquakes, Geophys. Bull. Hokkaido Univ., 13, 99-103

Wesnousky S and Scholz C (1983) Earthquake frequency distribution and the mechanics of faulting, Jour. Geophysics. Res., 88, 9331-9340

Wys M (1973) Toward physical understanding of earthquake frequency distribution, Geophys. Jour. Res. Astr. Soc., 31, 341-359

Ziegler M A (2001) Late Permian to Holocene paleofacies evolution of the Arabian plate and its hydrocarbon occurrences, GeoArabia, 6(3), 445-504.